

SOUTHERN CALIFORNIA PARTICLE SUPERSITE

Progress Report for Period August 1, 2001 - December 1, 2001

United States Environmental Protection Agency

Principal Investigator: John R. Froines, Ph.D., UCLA School of Public Health

Co-Principal Investigator: Constantinos Sioutas, Sc.D., USC School of Engineering

1. Introduction

The overall objective of the Southern California Particle Supersite is to conduct research and monitoring that contributes to a better understanding of the measurement, sources, size distribution, chemical composition and physical state, spatial and temporal variability, and health effects of suspended particulate matter (PM) in the Los Angeles Basin (LAB).

This report addresses the period from August 1, 2001 through December 1, 2001. It is divided into 13 sections each addressing a specific research area, including an update on a QA audit report. Furthermore, a major portion of the information included in this report has been either submitted or accepted for publication in peer-reviewed journals. Below is a list of manuscripts either submitted or accepted for publication which were produced through the Southern California Supersite funds and in which the EPA Supersite program has been acknowledged:

1. Misra, C., Geller, M., Sioutas, C and Solomon P. "Development and evaluation of a continuous coarse particle monitor". *Journal of Air and Waste Management Association*, 51:1309-1317, 2001
2. Geller, M.D., Kim, S. Misra, C., Sioutas, C., Olson, B.A and Marple, V.A. "Methodology for measuring size-dependent chemical composition of ultrafine particles" *Aerosol Science and Technology*, accepted for publication, October 2001
3. Misra, C., Kim S., Shen S. and Sioutas C. "Design and evaluation of a high-flow rate, very low pressure drop impactor for separation and collection of fine from ultrafine particles". *Journal of Aerosol Science*, accepted for publication, October 2001

4. Zhu, Y., Hinds, W.C., Kim, S and Sioutas, C. "Concentration and Size Distribution of Ultrafine Particles near a Major Highway". *Journal of Air and Waste Management Association*, accepted for publication, September, 2001
5. Singh, M., Jaques, P. and Sioutas, C. "Particle-bound metals in source and receptor sites of the Los Angeles Basin". Manuscript submitted to *Atmospheric Environment*, September, 2001.
6. Kim, S., Shi, S., Zhu, Y., Hinds, W.C., and Sioutas, C. "Size Distribution, Diurnal and Seasonal Trends of Ultrafine Particles in Source and Receptor Sites of the Los Angeles Basin". *Journal of Air and Waste Management Association*, accepted for publication, November, 2001
7. Miguel, A. H., Eiguren, A., Jaques, P and Sioutas, C.,. "PAHs in the Los Angeles Air Basin: Effects of Atmospheric Transport on Particle Size". Submitted to *Atmospheric Environment*, December 2001

2. PIU Sampling Location and Status

A key feature of our Supersite activities was the ability to conduct state-of-the-art measurements of the physicochemical characteristic of PM in different locations of the Los Angeles Basin (LAB). We have proposed a 2.5-year repeating cycle of measurements at five locations. Each location will be sampled during a period of intense photo-chemistry (defined approximately as May – October) and low photochemical activity (defined as the period between November – April). During this period, we have continued our PM sampling at Rubidoux, and have deployed the Particle Instrumentation Unit (PIU) to Claremont, our fourth sampling site, on September 12, 2001. Sampling at Claremont commenced during the week of September, and will continue through the winter of 2002. We have completed most of the chemical speciation analysis for integrated samples collected in Rubidoux, and some for Claremont, and as in Rubidoux, we have been conducting collaborative studies with outside investigators. For example, an "intensive" inter-lab comparison study has been conducted at Rubidoux during August 15 through September 8 2001. We have continued to make size-segregated on-line measurements of particulate nitrate using the Integrated Collection and Vaporization System (ICVS) developed by Aerosol Dynamics Inc. (ADI), and have installed and are currently validating their ICVS Carbon monitor. We have also been conducting field validations of two sets of prototype TEOMS (SES, and FDMS) in collaboration with R&P (Albany, NY).

Additionally, health studies have been conducted at Rubidoux and Claremont, of which particulate measurements have been made to support the studies that investigate exposure effects. The following health studies have been supported by the Supersite measurements:

1. In vitro studies undertaken by Drs. Andre Nel and Arthur Cho (UCLA) and Robert Devlin (US EPA) investigating the hypotheses that organic constituents associated with PM, including

quinones, other organic compounds (PAHs, nitro-PAHs, and aldehydes/ketones) and metals, are capable of generating reactive oxygen species (ROS) and acting as electrophilic agents

2. Animal inhalation toxicology studies using Concentrated Ambient Particulates (CAP) investigating the hypotheses that atmospheric chemistry is important in the toxicity of PM and co-pollutants, airway injury and cardiovascular effects will be greater at receptor sites downwind of source sites along the mobile source trajectory in the Los Angeles basin. These studies are led by Drs. Harkema (University of Michigan), Kleinman (UC Irvine), Froines and Nel (UCLA)

3. Time Integrated Size Fractioned Chemical Speciation for Riverside & Rubidoux

Our current sampling scheme involves the use of three MOUDIs for 24-hour averages: size-fractionated measurements of ambient and concentrated PM mass and chemical composition. Sampling is conducted once a week, on a Tuesday, Wednesday or Thursday, in order to coincide with one of the sampling days of the AQMD speciation network (which takes place every 3rd day). However, during “intensive” particulate characterization studies and for our support of co-located health effects exposure studies, we follow sampling schedules that are consistent with these special studies. Typically, ambient data are averaged over 24 hours, whereas for exposure or source contribution measurements, the time integrals may vary.

In each run, consistent with our original Supersite proposal, we have used three collocated Micro-Orifice Uniform Deposit Impactors (MOUDI) to group PM into the following size ranges:

- <0.1 μm (ultrafine particles)
- 0.1- 0.32 μm (accumulation mode, “condensation” sub-mode)
- 0.32 -1.0 μm (accumulation mode, “droplet” sub-mode)
- 1.0-2.5 μm (“intermediate” mode)
- 2.5-10 μm (coarse particles)

In addition to mass concentration, the following chemical components have been analyzed within these size groups:

- a. inorganic ions (i.e., sulfate, nitrate, ammonium)
- b. trace elements and metals
- c. elemental and organic carbon (EC/OC) content
- d. concentrations of polycyclic aromatic hydrocarbons (PAH)

One of the major objectives of the Supersite is to investigate the physiochemical differences between PM source and receptor locations within the Los Angeles basin. Normally, “condensation” particle growth occurs rapidly, and Downey, which is immediately downwind of the 710 Freeway, has the greatest heavy engine diesel truck traffic density in Los Angeles (about 30 to 40% of total vehicles, at any one time), while the Riverside and Rubidoux sites do not, and are several miles downwind (about

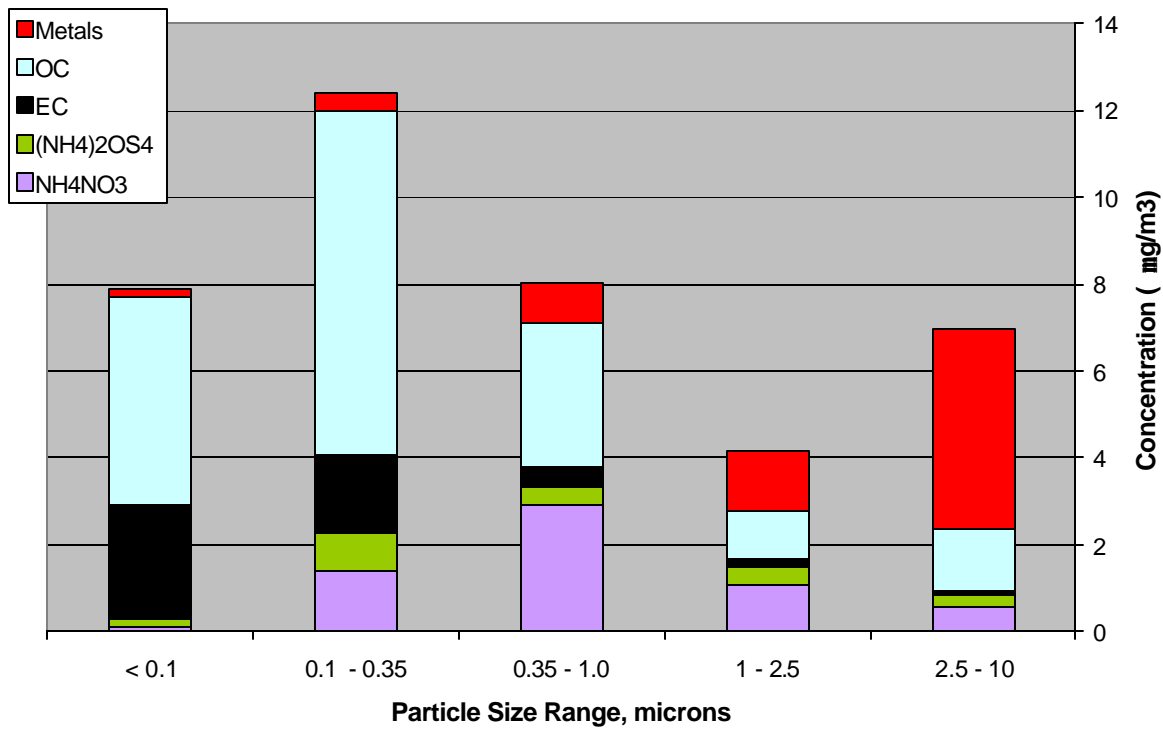
40 to 50). Under these conditions, it may be expected that ultrafine particles emitted at the freeway source grow to the condensation sub-mode, measured at Downey, while the larger particles (droplet sub-mode, and coarse mode) at Riverside and Rubidoux are from different sources.

Filter samples are also chemically speciated, in part, to: determine the source receptor trajectory profile, and to provide information for other Supersite related health studies within the SCPCS and for the NARSTO archives. Organic Carbon (OC) is a direct primary emission product from mobile sources, especially diesel. During and immediately after the combustion process, it may act as a nuclei particle (i.e., within the “ultrafine” size range). Semi volatile organic carbon (SVOC) compounds may condense onto the nuclei, thus forming the condensation sub mode. Additional collisions with water molecules and further condensation of SVOCs and water vapor can generate larger particles (i.e., in the “droplet” mode). Ammonium Nitrate (NH_4NO_3) associated air pollution particles can be formed by the reaction of Ammonia (NH_3) gas and primary and secondary translocated NO_x emissions. They tend to predominate in the 2.5 micro-meter fraction of particulate matter. Figures 1 - 3 present MOUDI collected mass concentrations, by chemical group, at both sites. Much higher levels of OC, in the PM_{10} fraction (about $17 \mu\text{g}/\text{m}^3$), have been measured in Downey, compared to about $9 \mu\text{g}/\text{m}^3$ in Riverside and Rubidoux. In comparison, particulate NH_4NO_3 levels are predominantly greater in Rubidoux ($14 \mu\text{g}/\text{m}^3$) and Riverside ($9 \mu\text{g}/\text{m}^3$), then in Downey ($5 \mu\text{g}/\text{m}^3$). This is expected, as Rubidoux is immediately downwind of a dairy farm, while Riverside is also, but further east by about 5-7 miles. The results also show that OC dominates all other chemical species in the PM_{10} fraction in Downey, while NH_4NO_3 dominates the droplet sub-mode at Riverside and Rubidoux.

The size distribution for total chemical mass is bimodal for all sites, with the smaller mode predominating in the condensation sub-mode in Downey, and in the droplet sub-mode in Riverside and Rubidoux. Within the Fine PM fraction: 1) at Downey, OC dominates other species in its contribution to the condensation mode; 2) at Riverside, NH_4NO_3 and OC equally contribute to the droplet mode; and 3) at Rubidoux, NH_4NO_3 is the primary contributor to the droplet mode. All 3 sites also have a coarse mode, dominated by metals, but in much greater concentrations in Riverside ($7 \mu\text{g}/\text{m}^3$) and Rubidoux ($14 \mu\text{g}/\text{m}^3$). The metals at Downey ($\sim 5 \mu\text{g}/\text{m}^3$) are primarily from locally re-suspended road dust, and those at Riverside and Rubidoux are mostly alkali (see Section 10, below), and are from locally suspended soil. Since Riverside and Rubidoux are in the desert environment, it is expected that they may be higher. In addition, Rubidoux is much greater than Riverside, very likely, because these measurements took place while the PIU was located at Riverside in the late winter and spring, while it was at Rubidoux throughout the summer.

Figure 1. Geometric means of 24-hour averaged size distributions of size speciated chemical mass, measured by the MOUDI at Downey.

24-h Average PM10 Mass and Chemical Composition in Downey



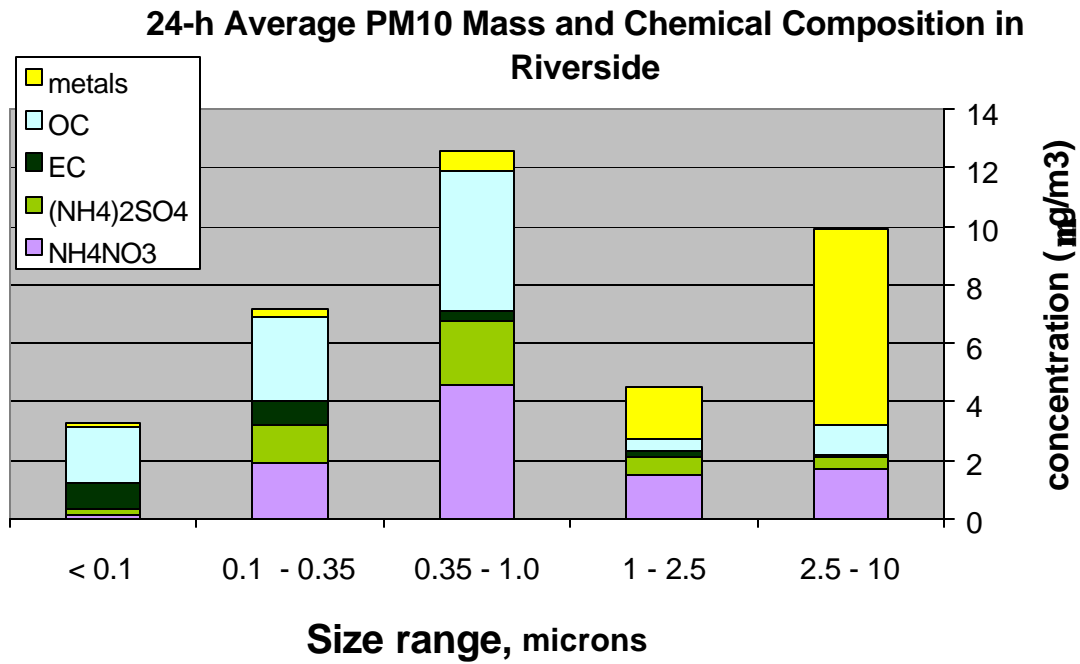


Figure 2. Geometric means of 24-hour averaged size distributions of size speciated chemical mass, measured by the MOUDI at Riverside.

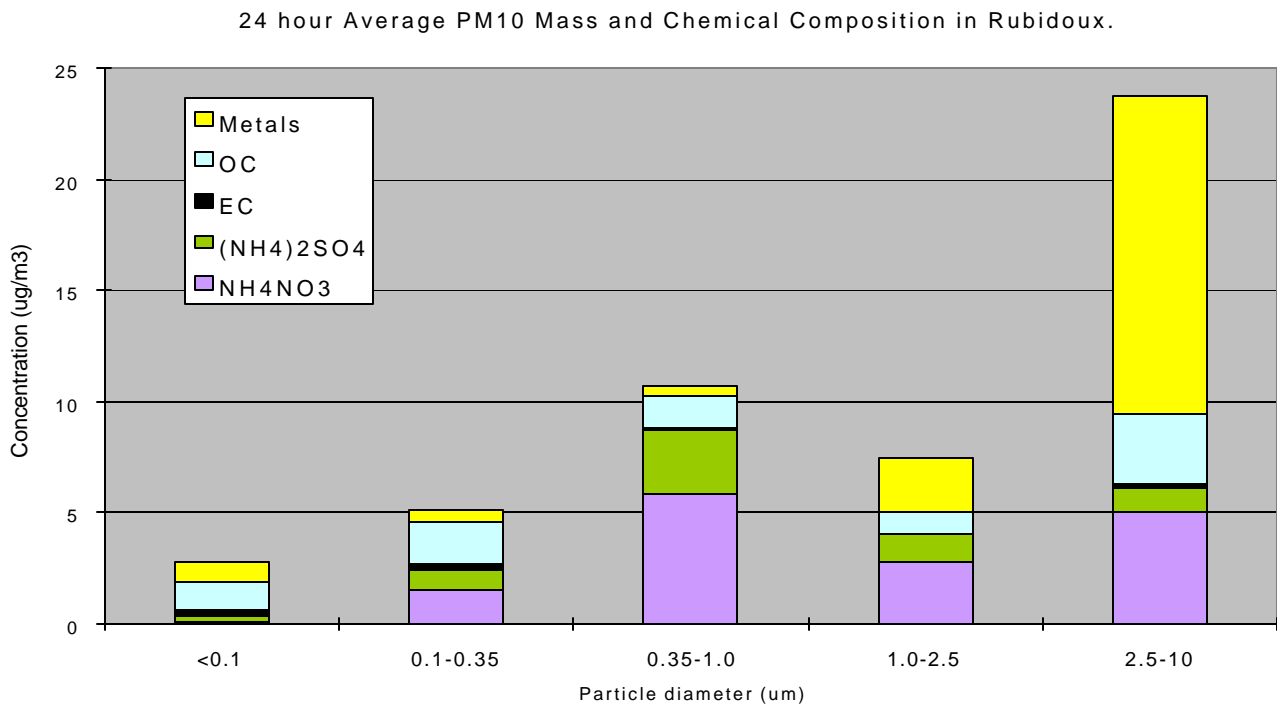


Figure 3. Geometric means of 24-hour averaged size distributions of size speciated chemical mass, measured by the MOUDI at Rubidoux

4. Comparison of FRM PM_{2.5} and PM₁₀ with SMPS-APS, TEOM and MOUDI

Introduction:

The SMPS and APS have originally been designed to characterize aerosols in the laboratory. More recently, they've been applied in field studies to investigate size distributions of ambient particulate matter on a semi-continuous time scale (e.g., 10 to 15 minute time integrals). We have operated the SMPS and APS in tandem; sampling through the same inlet to minimize diffusion based losses. Both instruments sample into small size bins, by number concentration. We have determined the mass concentration for various size fractions (e.g., PM_{2.5} and PM₁₀) and have compared these measurements to that of filter-based mass measurements, in part to evaluate the utility of the SMPS-APS as a continuous mass monitor for the convenience of obtaining greater time resolution data for health based and source apportionment studies.

In the presented set of measurements, to more closely track the semi-continuous Mass of the SMPS-APS monitors, diurnal and 24 hour filter based mass measurements are compared: 1) 6am – 10am; 2) 10am – 3pm (Downey), or 4pm (Riverside); 3) 3 or 4pm – 8pm; and 8p – 6am. SMPS-APS particle mass (< 10 μ m, and < 2.5 μ m) was determined by integrating the cumulative number count for these size fractions, and converting to volume by assuming a average LA basin particle density of 1.6.

Equipment:

- Continuous PM monitors:
 - TEOM
 - SMPS-APS

- Reference Gravimetric Samplers:
 - Dichotomous Partisol (PM-10 FRM inlet): PM₁₀, Coarse & Fine PM
 - MOUDI.

Methods:

- Diurnal Integrated Filter Measurements vs. Continuous Mass Measurements
 - Riverside: One week in May
 - 6a-10a, 10a-4p, 4p-8p, 8p-6a
 - Daily Integrated Filter Measurements vs. Continuous Mass Measurements
 - Downey, Riverside, and Rubidoux

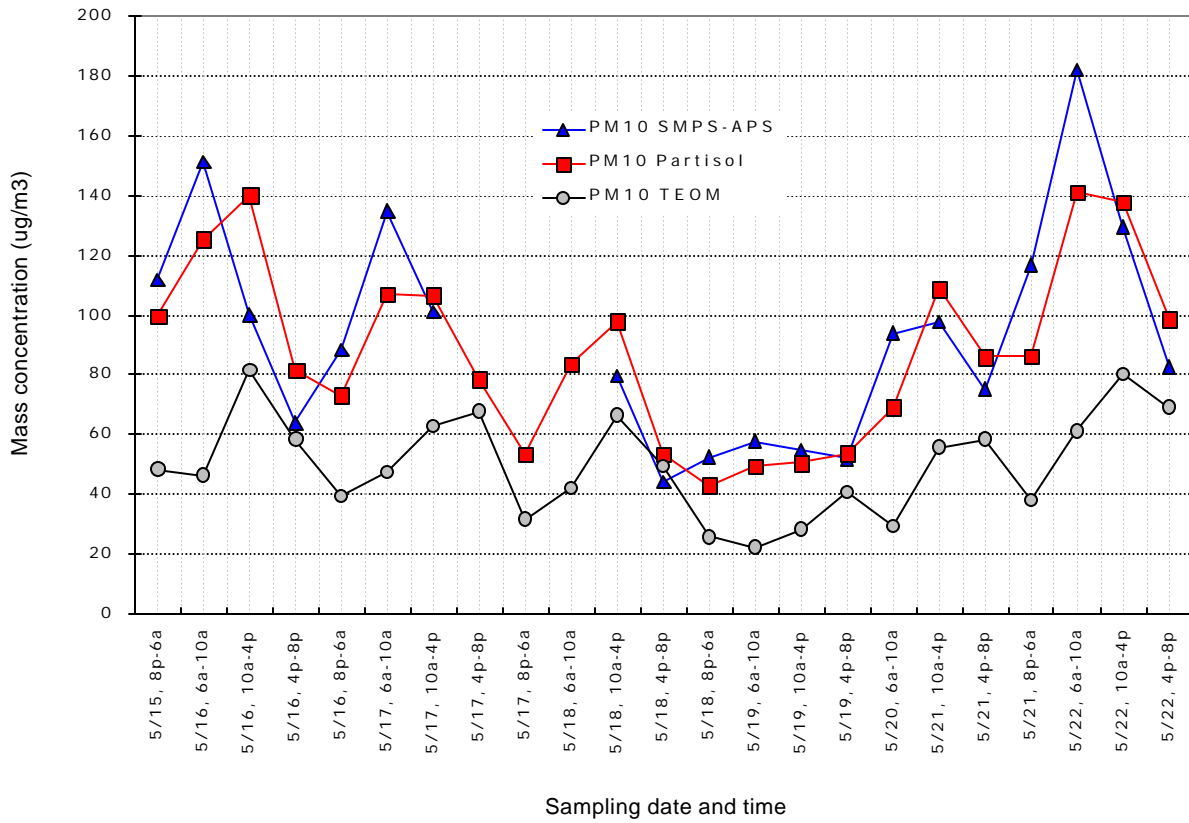
- Co-located Inter-comparisons
 - Downey: SMPS-APS vs. MOUDI & FRM

- Riverside: SMPS-APS vs. TEOM & FRM

Results and Discussion:

Figures 1 and 2 present the diurnal measurements conducted at Riverside. In general, the SMPS-APS system closely tracks both the FRM and TEOM over time, and is very highly correlated ($R^2 = 0.93$) with the FRM - having a slope of nearly one. The consistently lower TEOM measurements are most likely due to our using the heated version of the TEOM (1400a) at that time, resulting in volatile chemical desorption losses. A lag trend appears possible, with the TEOM peaks following those of the SMPS-APS. The SMPS-APS measures particles in near “real time”, and the TEOM records the mass of an oscillating filter every 10 minutes, which may result in a delayed loss of mass that may not be recorded until the next time integral – thus, possibly contributing to a “lag effect”. This potential phenomenon will be examined more closely for publication purposes.

Figures 3 compares 24 hour integrated filter Fine mass measurements by the Partisol & MOUDI to that of the SMPS-APS system for the 3 sites between Oct 3, 2000 and July 18, 2001. The integrated filter mass samplers (MOUDI and Partisol) track the semi-continuous SMPS-APS sampler very closely. Figures 4 presents a scatter plot of the PM_{2.5} mass between the same instruments. Both the Partisol ($R^2 = 0.70$) and MOUDI ($R^2 = 0.90$) are highly correlated with the SMPS-APS. On average, the Partisol and MOUDI concentrations are about 84 and 80% of the SMPS-APS, respectively, most likely because time allows for semi-volatile loss of PM from the integrated filter samples, while the SMPS-APS measures particle counts in real-time. In addition, the APS may measure a small fraction of small particles as artifacts, potentially contributing to a significant mass of the larger particles (Armendariz and Leith, *J. of Aerosol Sci.*; 33 (2002) 133-148).



Figures 1. PM10 Mass Sampled by Partisol, TEOM and SMPS-APS LA Supersite: Riverside (May 2001)

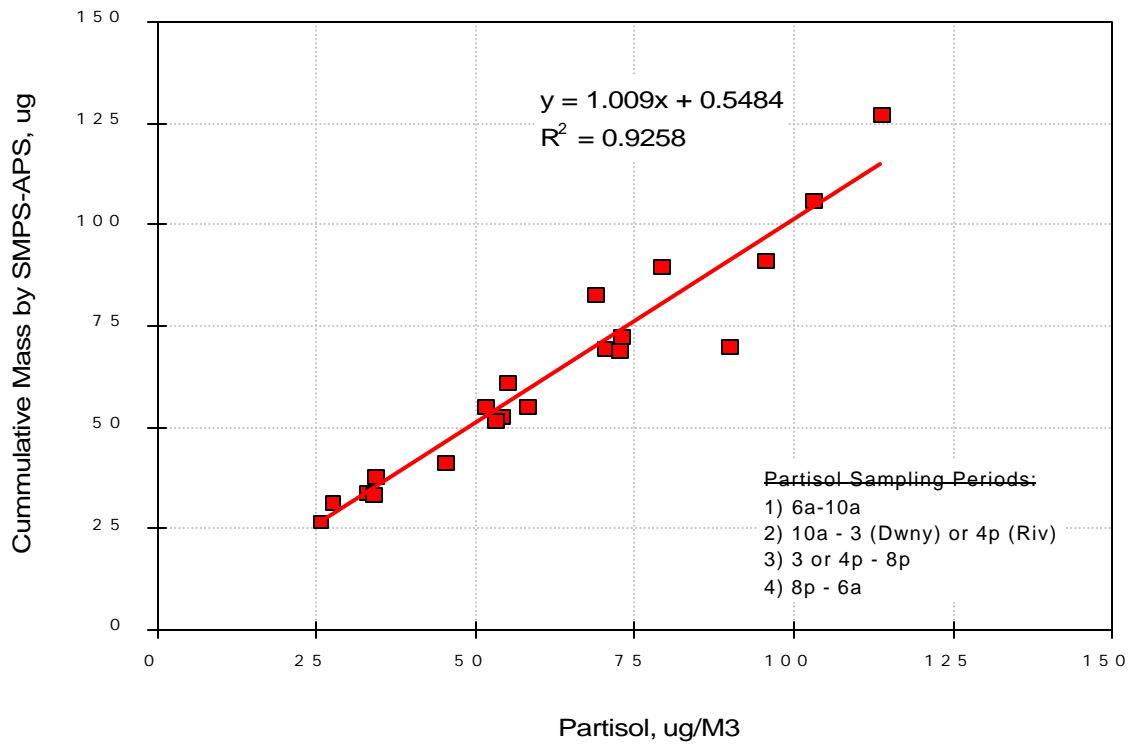


Figure 2. Comparison of PM2.5 Mass Simultaneously Sampled by Partisol and SMPS-APS LA Supersite: Riverside (May 2001)

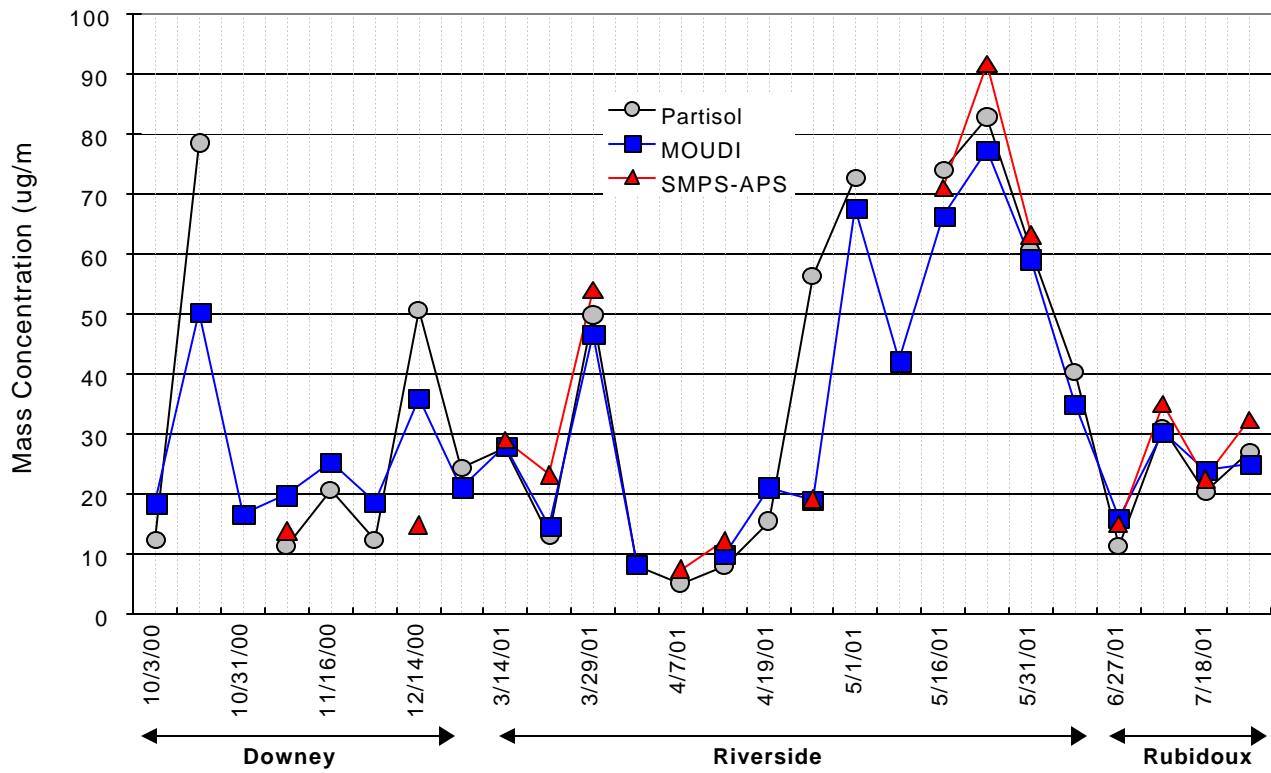


Figure 3. Daily PM2.5 Mass by SMPS-APS, Partisol and MOUDI LA Supersite Locations: Downey, Riverside, & Rubidoux.

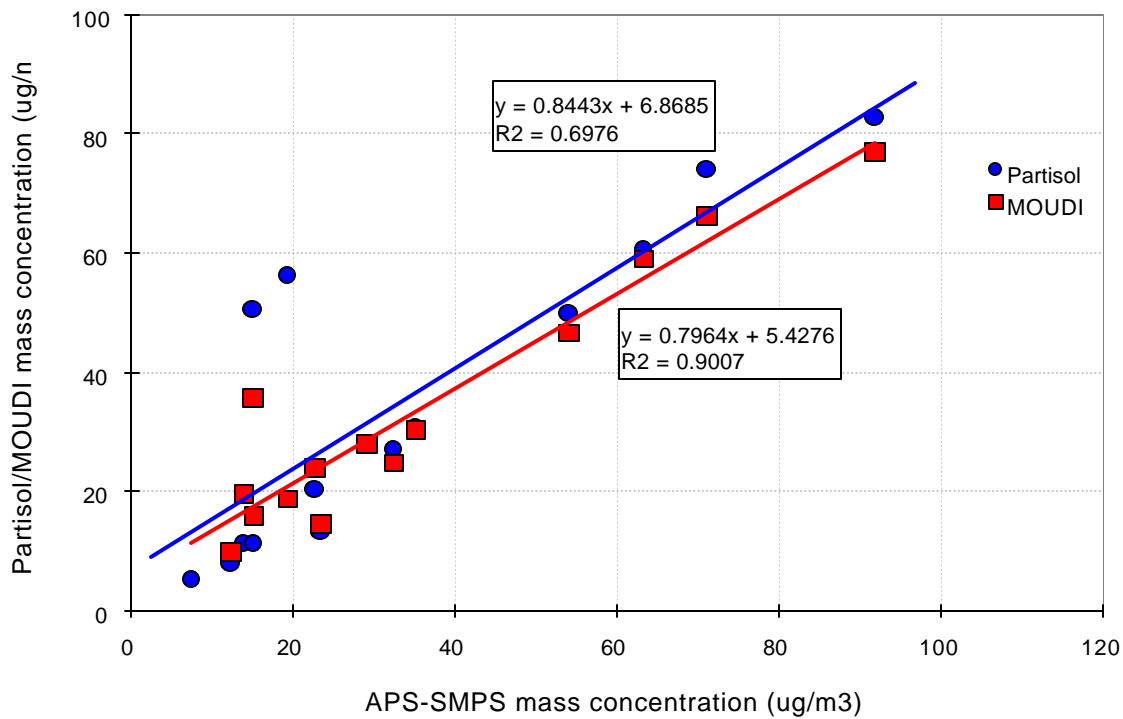


Figure 4. PM2.5 Mass concentration comparison between Partisol & MOUDI to the SMPS-APS LA Supersite: Downey, Riverside, Rubidoux (Oct 2000 - July 2001).

5. Comparison of EC by the Aethalometer to Filter-based Measurements

For several years, the Aethalometer (Hansen, et al., 1984) has been used to measure Black Carbon (BC) as a surrogate for Elemental Carbon (EC) - a combustion bi-product. Particles are sampled onto a quartz filter tape that upon sufficient loading, as measured by reduction in light absorption, is automatically transported to commence a new sample integral (typically 1 to 3 hours). The reduction in light (wavelength = 880 nm) through the continuously blackening filter is converted to EC mass via a previous standard-light calibration, and is recorded to disk at 5-minute intervals (i.e., semi-continuously). It has been reported that the efficiency of the Aethalometer may vary with fresh and aged (i.e., transported) particles, as a function of particle size (Allen, et al., 1998; and, Babich, et al., 2000).

During the course of the Supersite program, we have operated the Aethalometer (Model AE-20UV) on a regular basis, and, herein, are reporting comparisons to co-located filter based measurements, analyzed by the thermal optical desorption technique (Sunset Labs). Measurements were conducted in Downey (December, 2000 through February 1, 2001), the LA Supersite mobile source site, heavily occupied by diesel truck traffic, and at Riverside (March through June 2001), about 50 miles downwind, and subject to a much lower density of traffic. At Downey, diurnal co-located measurements with the FRM are made, and at Riverside, 24 hour integrated measurements are compared to those by the MOUDI.

Results and Discussion:

At Downey, EC measured by the Aethalometer tracks the Partisol very closely for PM_{2.5} (see Figure 1). Comparisons between the two methods show that EC measured by the Aethalometer is dominant in the PM_{2.5} fraction, but that the coarse fraction is approximately 10 to 15 % of the total EC mass measured by the Aethalometer (Figures 2). Figure 3 presents 24 hour integrated EC mass measurements at Riverside (the downwind site), made during the spring, and compared to the MOUDI, rather than the FRM. Overall the MOUDI tracks the Aethalometer over the course of these measurements (3 months), but is about 70% of the PM_{2.5} mass, on the average. In contrast to Downey, there is much more EC in the PM_{2.5} fraction at Riverside (about 95%, on the average). Figure 4 presents the size segregated EC measurements made by the MOUDI. On the average, about 80 to 95% of EC is in the sub-micron fraction, and depending on the day, may predominate in the ultrafine, condensation, or droplet sub-modes. A more detailed analysis of the relationship of wind direction and velocity to these modes will be conducted to evaluate EC source contributions. For direct comparison between the two sites, there exists fewer size segregated MOUDI measurements at Downey, but the existing data will be further analyzed to compare with that of Riverside. We will compare the relative proportions of EC in the ultrafine and sub-micron modes in order to investigate whether aged particles may have a different response to the optical absorption technique used by the Aethalometer than the analysis of the integrated filter samples, via thermal desorption. The mass-to-absorbance relationship may vary with the size distribution of fresh and aged particles as argued by Babich, et al., 2000. In addition, other compounds that may adsorb onto the carbon particles may act as artifacts for the Aethalometer, and possibly the thermal desorption technique.

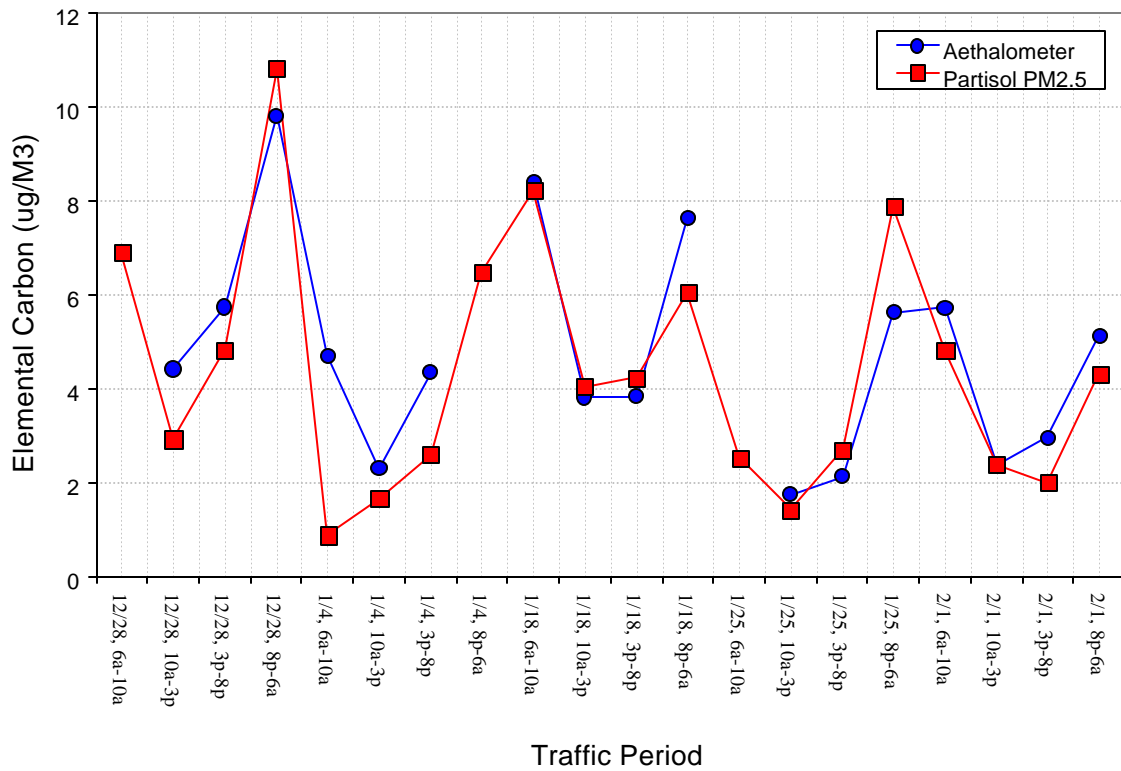


Figure 1. EC by Aethalometer vs PM-2.5 EC by Partisol during Distinct Time Periods LA Supersite: Source Site - Downey, CA (Dec 2000 to Feb 1, 2001)

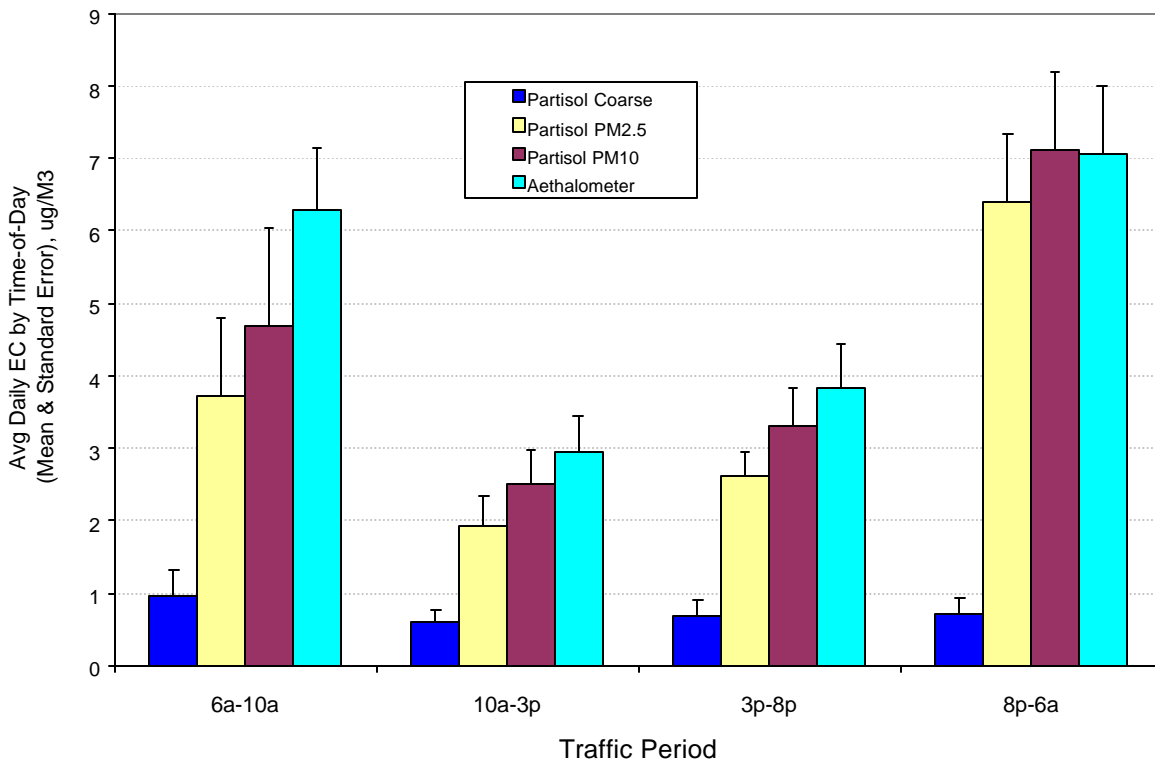


Figure 2. Average Daily EC by Aethalometer & Partisol during Distinct Time Periods LA Supersite: Source Freeway Site - Downey (Dec 2000 - Feb 2001)

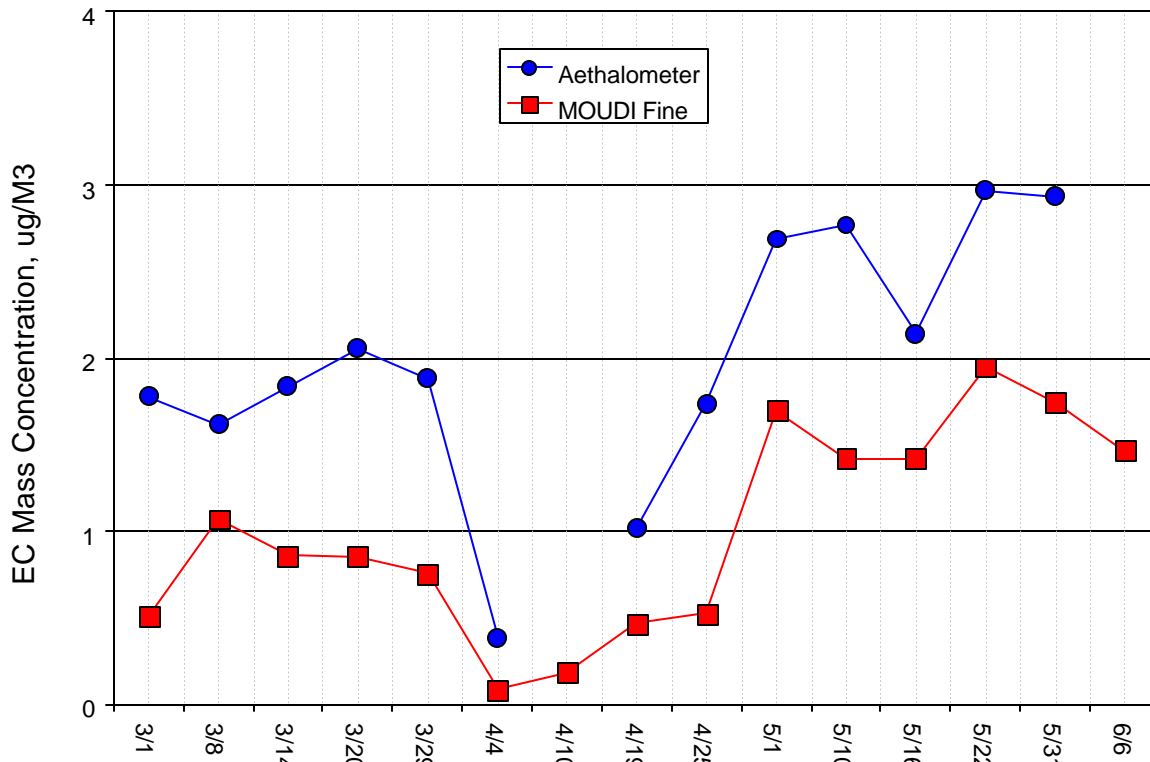


Figure 3. Daily EC by Aethalometer and PM_{2.5} EC of MOUDILA Supersite: Riverside (March - June 2000).

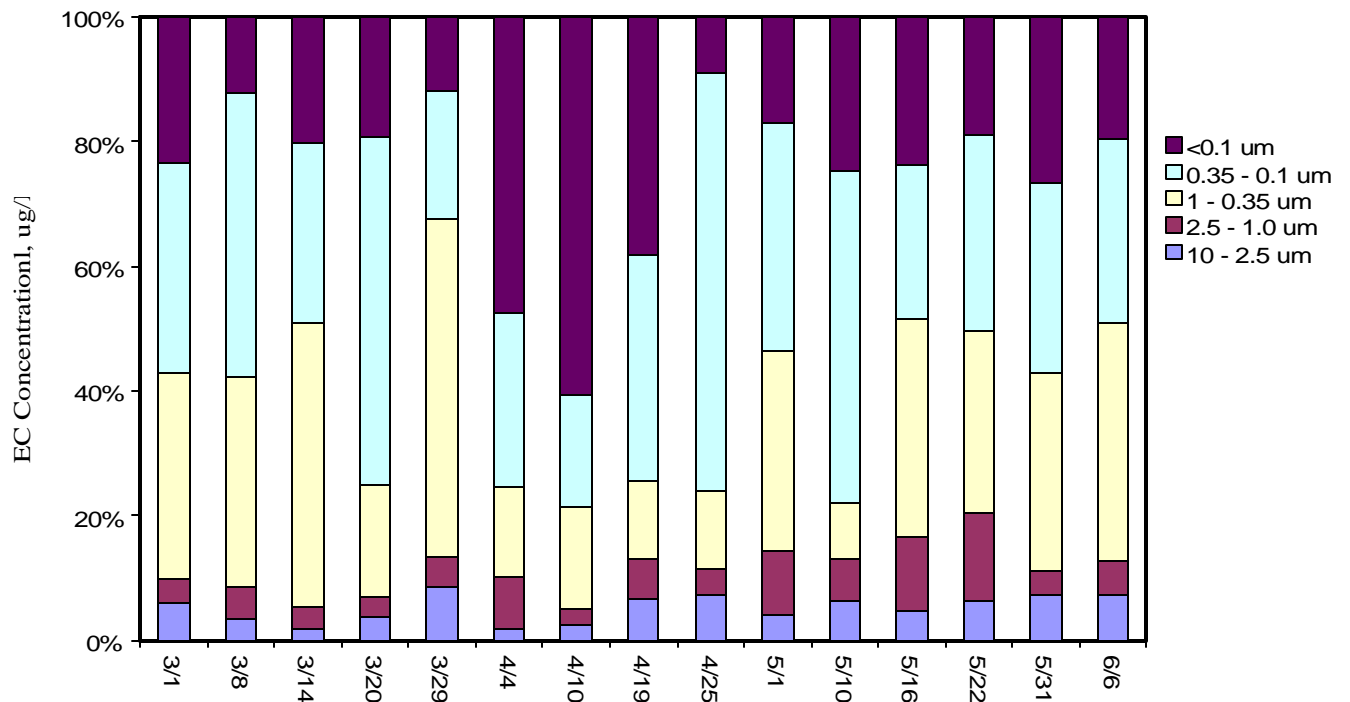


Figure 4. Relative EC by Size Fraction, Measured by MOUDI Impactor Spring 2001, LA Supersite: Riverside, CA.

6. Size-segregated on-line measurement of particulate carbon and nitrate using the Integrated Collection and Vaporization System (submitted 12/5/2001)

During this quarter size-resolved particulate nitrate concentration data have been collected by Aerosol Dynamics Inc. with the Integrated Collection and Vaporization System (ICVS) from both the Rubidoux (7/12/01-9/12/01) and Claremont (9/14/01-present) sites of the UCLA Particle Instrumentation Unit (PIU). The particulate Carbon ICVS was installed in Claremont on 10/10/2001, but has collected incomplete data due to carrier gas issues.

The Carbon ICVS is very similar to the Nitrate ICVS. The general ICVS measurement approach utilizes a 2.5 μm precut and successive impaction stages to collect three particle size fractions. The sample is humidified to prevent particle bounce. Stage A collects particles from 1.0 to 2.5 μm at 65% RH, Stage B from 0.45 to 1.0 μm at 65% RH, and Stage C from 0.14 to 0.45 μm at \sim 90% RH. After collection, the cells are sequentially flushed with carrier gas and the samples vaporized by flash volatilization (i.e. rapid resistive heating). The now gaseous sample is carried downstream to a standard gas analyzer. The Carbon ICVS uses platinum impaction strips, CO_2 -free air carrier gas, a CO_2 analyzer downstream of a quartz oven set to 650 C, and runs on a 30 minute cycle. The Nitrate ICVS uses nichrome impaction strips, N_2 carrier gas, a NO_x analyzer, and runs on a 10 minute cycle.

The Nitrate ICVS humidity control system developed a problem in the field. Humidified air from outside the instrument was no longer saturated after entering the warmer instrument enclosure, resulting in humidities well below the 65% target. The humidity control system was modified for the Carbon ICVS by bringing the humidification bottle inside the instrument enclosure. This has stabilized the conditioned humidity in Stages A and B (see Fig. 1). Modifications have not yet been made to the Nitrate ICVS.

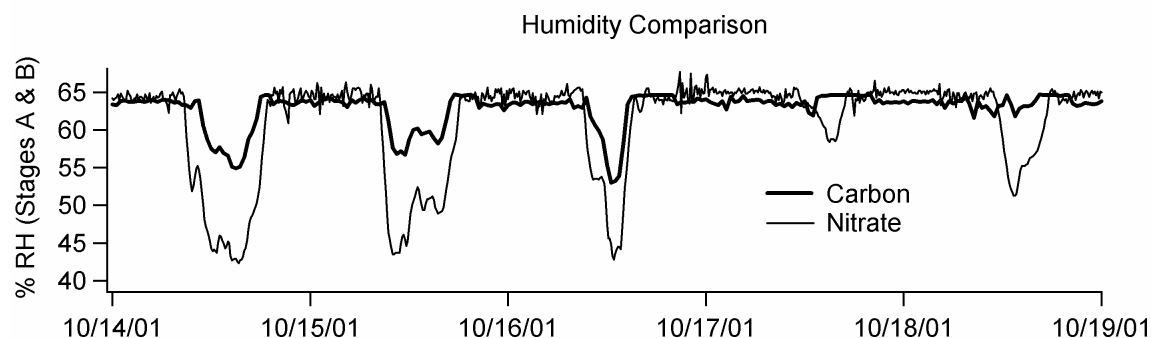


Fig 1: Comparison of the performance of the controlled humidity system between the original nitrate system and the updated carbon system.

Preliminary comparison of particulate nitrate data between the Rubidoux and Claremont sites reveals some interesting points (Figure 2). Both sites exhibit a pronounced peak during daylight hours beginning roughly at sunrise. This points to a formation mechanism involving photolysis such as photolytic

formation of OH, then $\text{OH} + \text{NO}_2 \rightarrow \text{HNO}_3$. The Claremont data show a more sustained peak throughout the day than the Rubidoux data, as well as a sharper rise in morning concentrations.

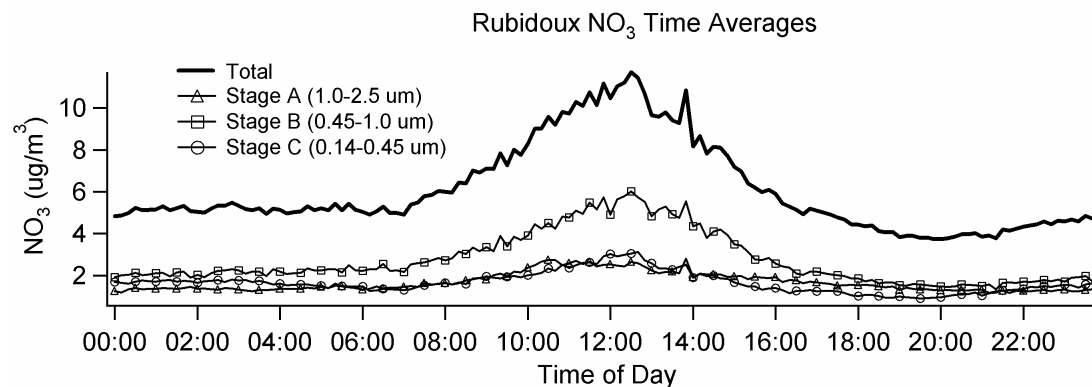


Fig 2A: Time averages of size-segregated particulate nitrate measurements in Rubidoux, CA from 7/12/01 to 9/12/01.

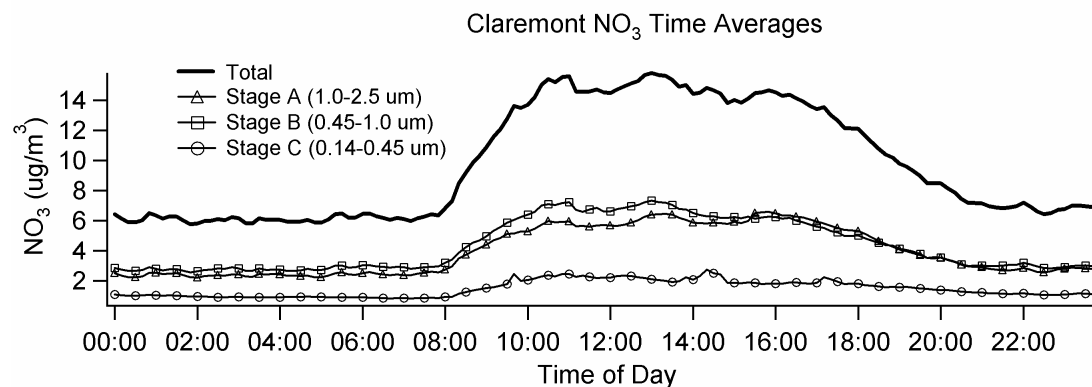


Fig 2B: Time averages of size-segregated particulate nitrate measurements in Claremont, CA from 9/14/01 to 11/27/01.

Stage B (0.45-1.0 μm) and Stage C (0.14-0.45 μm) concentrations are comparable at the two sites. Stage A (1.0-2.5 μm), corresponding to the coarse mode, is significantly higher at Claremont than Rubidoux. Analysis of these size and time-of-day trends with relation to local topography and weather patterns could yield further insight into nitrate formation mechanisms.

The Carbon ICVS was installed in Claremont on 10/10/01. Valid data were only collected from 10/10/01 to 10/21/01. A CO_2 scrubbing system was employed to remove CO_2 from ambient air pressurized by an on-site compressor. This system has proved inadequate, and the very high resulting baseline in the CO_2 analyzer overwhelmed the particulate carbon signal. Bottled industrial air will be substituted to remedy this issue. The system is currently shut down.

Three days of representative particulate carbon data are shown in Figure 3. Again, a marked increase can be seen in the morning hours near sunrise, suggesting photolytic particle formation mechanisms. The smallest size fraction (Stage C) dominates the mass concentration, Stage B increases only at high overall concentrations, and Stage A hardly changes at all.

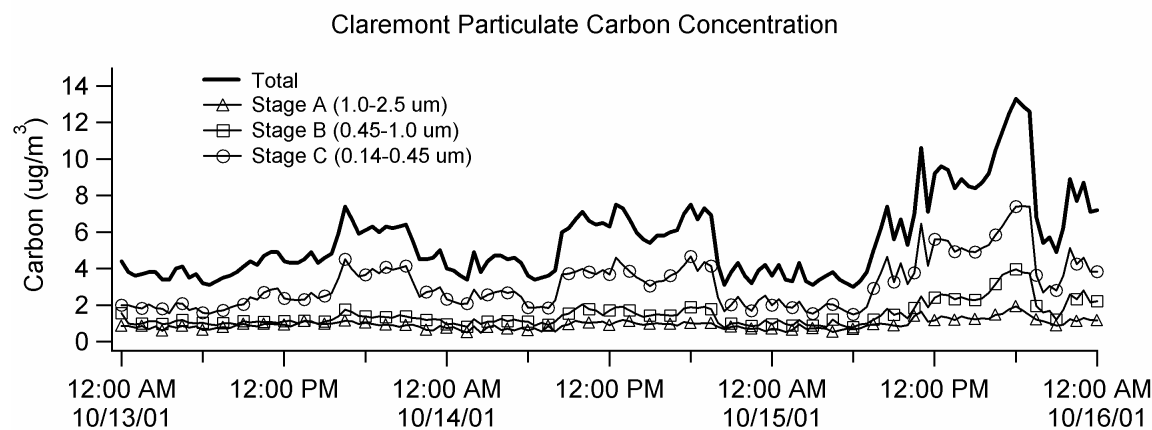


Fig 3: Size-segregated particulate carbon concentration from Claremont, California.

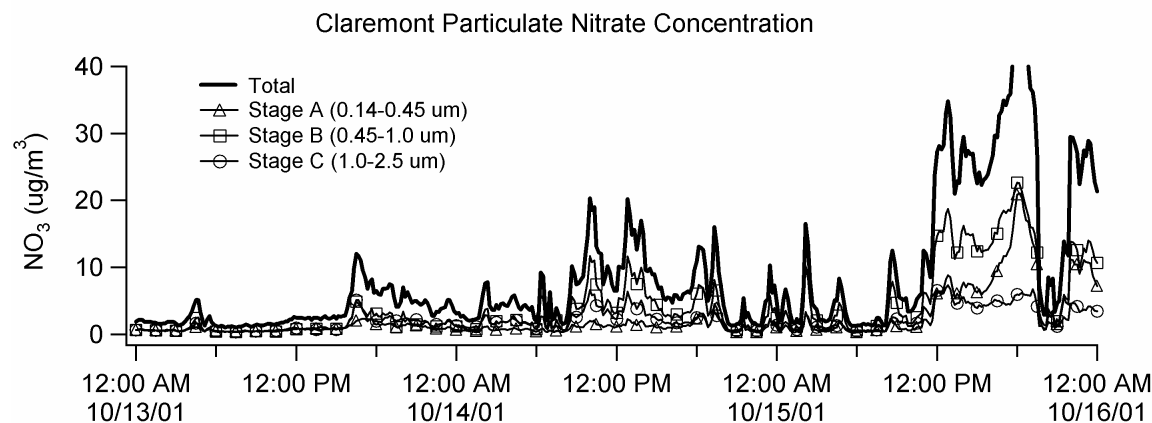


Fig 4: Size-segregated particulate nitrate concentration from Claremont, California.

The same three-day period is plotted for particulate carbon in Fig. 3 and particulate nitrate in Fig. 4. Concentrations generally rise and fall together as part of larger scale particle formation episodes. This assertion is also supported by a preliminary look at APS/SMPS particle distribution data contour plots supplied by Yifang Zhu and Peter Jaques.

Sampling will continue at the Claremont site. The Carbon ICVS will be restarted once bottled air is delivered to the site. Periodic visits will be made by Aerosol Dynamics staff for instrument calibration and maintenance.

7. Comparison of Polycyclic Aromatic Hydrocarbon Particle Size and Phase Distribution Near a Source (Downey) and at a Downwind Receptor Site (Rubidoux) in the LA Basin

Summary of the activities

During the report period, particle size and vapor-particle partition data for fifteen priority polycyclic aromatic hydrocarbons (PAH) were obtained from samples collected during a five-week experiment conducted during the summer in Rubidoux. This site is located downwind from Downey (strongly impacted by vehicular emissions) where a similar study was conducted in the Fall of 2000. In this report, a comparison is made of the size distributions and partitioning data obtained at both sites.

Introduction

Atmospheric transport moves the persistent organic species from their sources to downwind locations. During atmospheric transport, the fate of organics such as PAH is primarily governed by their chemical stability, vapor-particle partitioning, and size distribution. When partitioning occurs during transport, it may alter the size distribution of certain PAH leading to changes in their residence time, and, more importantly, in the efficiency of deposition in the human respiratory system.

Size distribution data for PAH with $\log [P^{\circ}_L] < -3.2$ (\geq MW 202) have been extensively reported in the literature for samples collected in roadway tunnels and ambient air using cascade impactors. However, size data for PAH that are found predominantly in the gas-phase (e.g. naphthalene, acenaphthene, fluorene, phenanthrene, and anthracene) are not available in the literature due to the low concentration found in the particle-phase, and the attended potential for sampling artifacts. To address the latter issue, Zhang and McMurry (1991) developed a theoretical model to examine evaporative losses that occur as a result of the pressure drop within a sampling device, assuming that temperature, gas, and particle concentrations remain constant during sampling. This model predicted that sampling efficiencies, when using vapor denuders upstream of filters, are always poorer than for impactors. On the other hand, for impactor sampling, the model predicted that evaporative losses of adsorbed or absorbed SVOC species collected may be large for those that are predominantly in the gas phase.

To evaluate this issue experimentally, we conducted a series of field experiments in two of the Southern California Particle Center and Supersite (SCPCS) sampling sites in the Los Angeles Basin: Downey, a site strongly impacted by vehicular emissions and in Rubidoux, ca. 30 km downwind. The sampling systems used are described below.

Experimental

Sample Collection: Size-resolved PAH were collected, during 24-hr periods, approximately every 7th day, beginning at 8:00 am, during a five-week field campaign conducted during the summer in

Rubidoux, starting August 23 and ending Sept 04, 2001. Samples from about 42 m³ of air were collected using co-located three-stage MOUDI impactors with three size cuts: < 0.18 μm (Mode I), 0.18-2.5 μm (Mode II), and 2.5-10 μm (mode III) aerodynamic diameter (dp). One MOUDI operated in the “regular mode”, and the other, with a vapor trapping system that included an XAD-4 coated annular denuder placed upstream of the impactor, and a polyurethane foam plug (PUF) placed in series behind the impactor.

PAH extraction and Chemical Analysis: Teflon filters corresponding to each size cut, the denuder and the PUF plug were extracted and analyzed separately by a highly sensitive HPLC-Fluorescence method developed in our lab and reported previously. Fifteen of the sixteen EPA priority PAHs were studied: naphthalene (NAP), acenaphthene (ACE), fluorene (FLU), phenanthrene (PHE), anthracene (ANT), fluoranthene (FLT), pyrene (PYR), benzo[a]anthracene (BAA), chrysene (CRY), benzo[b]fluoranthene (BBF), benzo[k]fluoranthene (BKF), benzo[a]pyrene (BAP), dibenz[a,h]anthracene (DBA), benzo[g,h,i]perylene (BGP), and indeno[1,2,3-c,d]pyrene (IND).

Results, Discussion and Conclusions

PAH particle-vapor distributions. An adsorptive partitioning model that predicts the vapor-particle distribution of SVOCs was developed by Junge (1977) and Pankow (1987)

$$\phi = c\theta / (P_L^o + c\theta)$$

where ϕ is the particle-bound fraction, θ is the particle surface area per volume of air, c is a constant dependent on heat of condensation and surface properties, and P_L^o the PAH subcooled liquid vapor pressure. Values of the particle-bound fraction (ϕ) predicted by the Junge-Pankow model for each of the target PAH using the Downy and the Rubidoux data (mean of $n=4$ and $n=5$ measurements, respectively) are plotted in Figures 1a-b. P_L^o values for IND are not available in the literature. The results show that, for fourteen PAH measured, the Junge-Pankow model fitted best when the vapor phase fraction was considered as the sum of PAH collected with the denuder and the PUF, and the particle-phase the sum of the mass collected on the Teflon filters. Consistent with literature data, at both sites, the fraction of PAH found in the particle-phase increases with decreasing P_L^o . However, while for samples collected in Downey the best model fit was obtained using a surface area per volume of air value of θ found for urban areas (Fig. 1a), for the receptor site samples the best fit was obtained using a θ value which is typical of background areas, reflecting a decrease in the particle surface area and changes in other surface properties occurring during transport.

PAH mass balances. For both sites, the sum of the PAH mass collected on the three stages of the MOUDI, with or without a denuder, showed good agreement (Figures 2a,b). Although for both sites the total mass collected with the regular MOUDI system was consistently larger than with the denuded MOUDI, the results obtained are not statistically different, an indication that sorption of gas-phase PAH onto sampled particle deposits is insignificant with the regular MOUDI configuration. For all

target species, mean total particle-phase PAH concentrations at the source site were on average 6 times larger than at the receptor site, especially for FLU and PYR which may have reacted to a larger extent during transport.

PAH size distributions. The size distribution of the fifteen PAH showed a larger mass fraction in Mode I for samples collected at the source site (Downey) and in Mode II at the downwind location, suggesting coagulation of Mode I particles into Mode II during atmospheric transport to Rubidoux (See Figure 3). For both the source and the receptor sites, the size distribution obtained using either regular or denuded MOUDI system are similar for the less volatile PAH ($\log [P^o_L] < -3.2$), but different for the more volatile PAH ($\log [P^o_L] > -3.2$). These differences may have resulted from the non-equilibrium conditions imposed by sampling with the denuded MOUDI configuration. Considering the good mass balances obtained for both MOUDI sampling systems, we may conclude that sampling using a regular MOUDI provides size distribution data that is not significantly affected by sampling artifacts.

In order to evaluate seasonal effects, similar experiments will be conducted during the winter.

Literature Cited

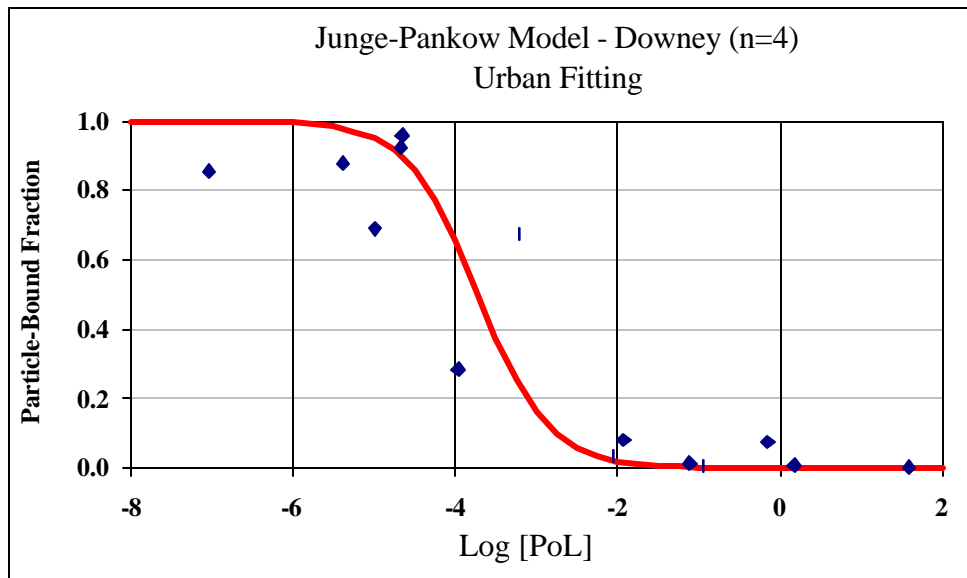
Junge, C. E. In *Fate of Pollutants in the Air and Water Environment*; Suffet, I. H., Ed.; Wiley-Interscience: New York, 1977; Part 1, Vol. 8, p 7-5.

Pankow, J. F. *Atmos. Environ.* 1987, 22, 2275-2283.

Zhang, X. Q, McMurry P. H, *Theoretical Analysis of Evaporative Losses of Adsorbed or Absorbed Species During Atmospheric Aerosol Sampling.* *Environ. Sci. Technol.*, 1991, 25, 456-459 1991

Figure 1. Junge-Pankow model fitting for PAH data collected in Downey (a) and Rubidoux (b)

(a)



(b)

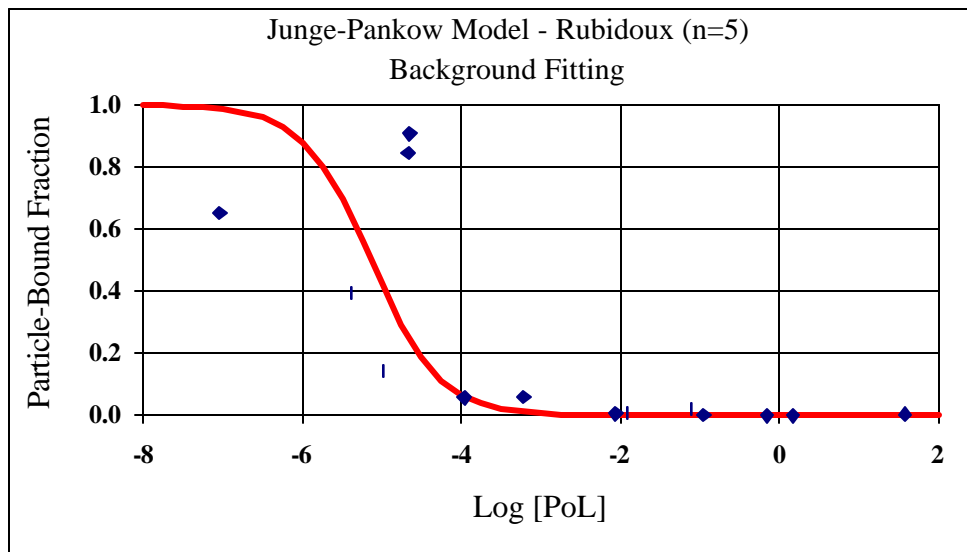
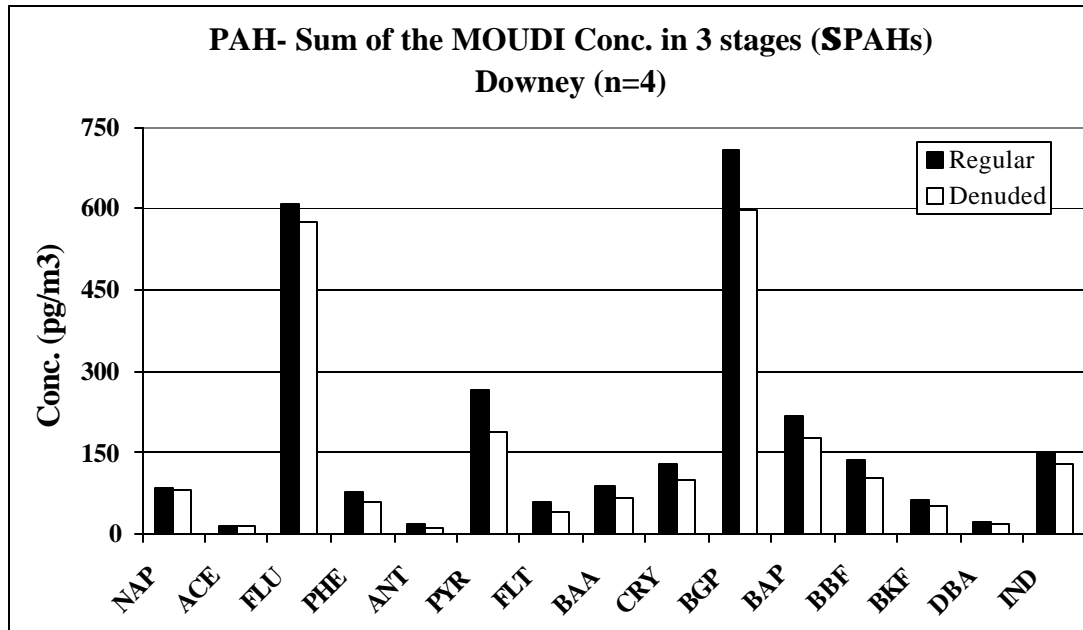


Fig 2. Mass balance of particle-phase PAH collected with regular and denuded MOUDIs in Downey (a) and Rubidoux (b)

(a)



(b)

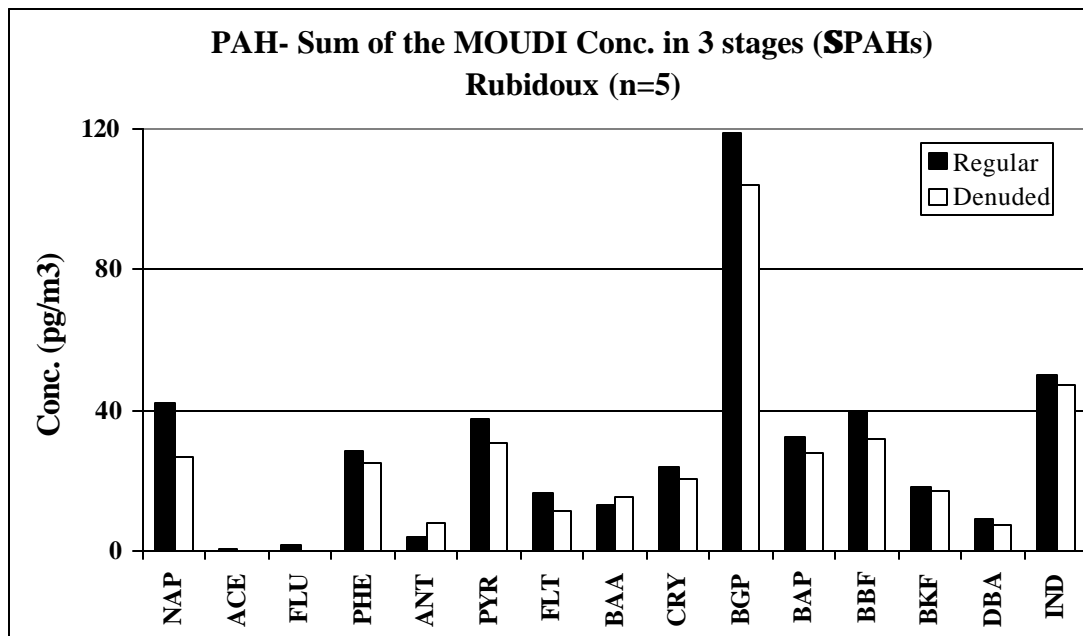
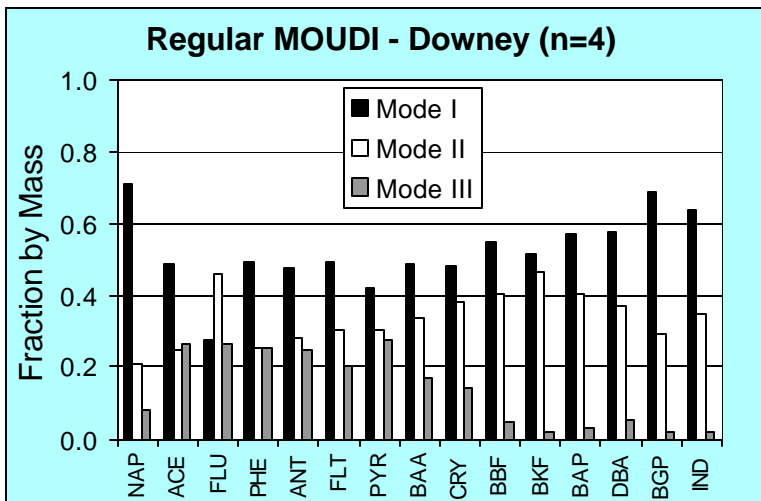
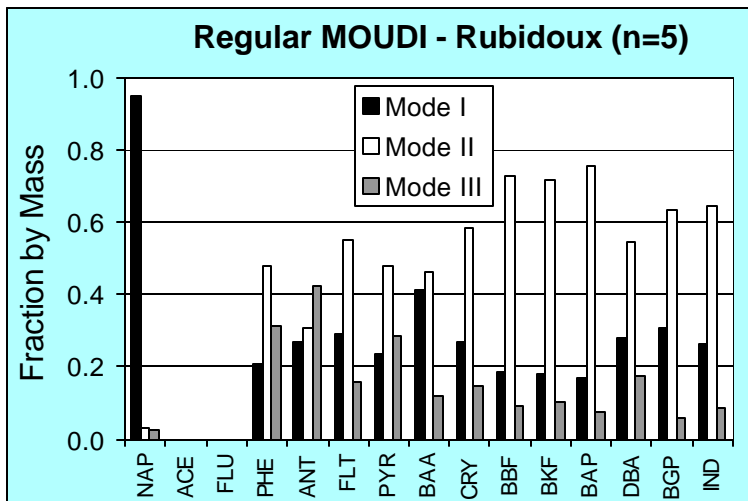


Figure 3. PAH size distributions obtained in Downey and Rubidoux with the regular (a,b) and the denuded MOUDI (c,d)

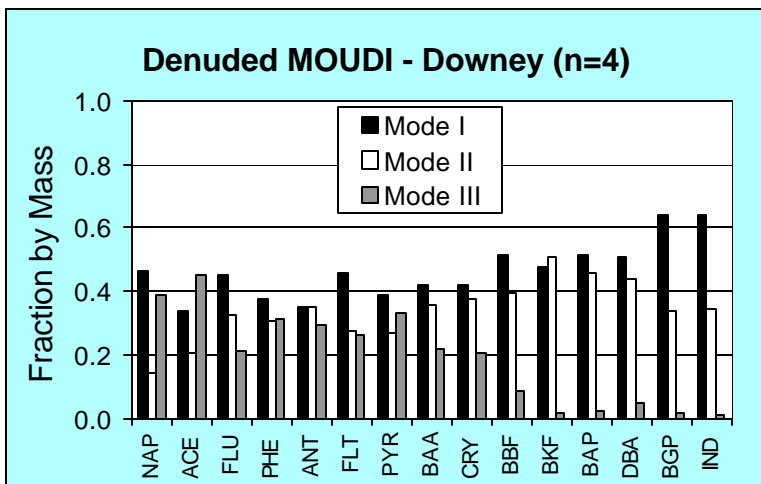
(a)



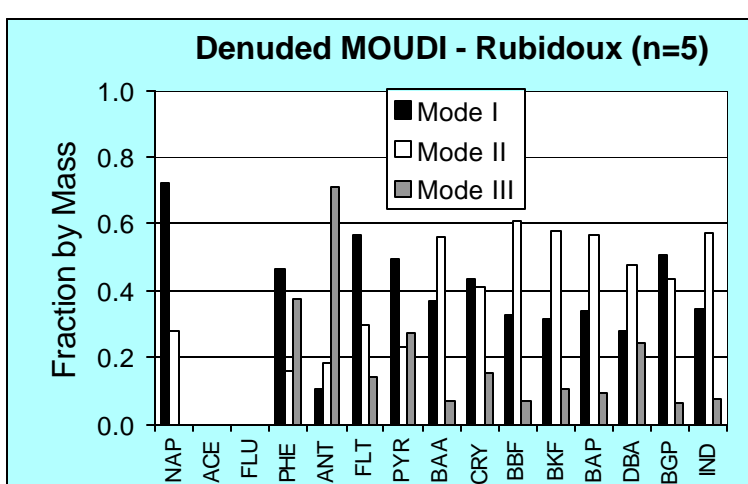
(b)



(c)



(d)



8. Measurements of Carbonyls in CHS Sites. Phase I: Atascadero, San Dimas and Riverside. Phase II: Lompoc, Mira Loma, and Upland

Summary of the activities

During the report period, carbonyls were determined in samples collected during phases I and II of the CHS in six of the twelve sites, including two background locations Atascadero (ATA) and Lompoc (LOM), and four sites located downwind from Los Angeles: San Dimas (SD), Mira Loma (MRL), Upland (UPL) and Riverside (RV).

Introduction

Carbonyls play an important role in photo-oxidation reactions that take place in the troposphere. They constitute an important class of compounds that are mostly produced in the atmosphere by photochemical reactions, and include the toxic formaldehyde and other aliphatic and aromatic carbonyls. The present study is being conducted at sampling sites within the twelve Southern California communities participating in the CARB-sponsored Children's Health Study (CHS), a longitudinal respiratory health study of several thousand Southern California school children.

Experimental

Sampling of carbonyls was conducted during 24-hr periods, approximately every 8th day, during spring-summer and summer-fall seasons using 2,4-DNPH cartridges and analyzed following an HPLC-DAD method developed in our lab and described in a previous report.

Results, Discussion and Conclusions

Twelve carbonyls were quantified in all six locations, including formaldehyde (FOR), acetaldehyde (ACD), acetone (ACE), propionaldehyde (PRO), crotonaldehyde (CRO), 2-butanone (BUT), butyraldehyde (BUD), methacrolein (MET), benzaldehyde (BEN), valeraldehyde (VAL), m-tolualdehyde (MTO), and hexaldehyde (HEX). Concentrations reported have been corrected for sample blanks. Thus, the lowest reported values reflect the "net" level found, not the detection limit.

During phase I, conducted during the spring-summer period, the carbonyl concentrations at the background site (Atascadero) averaged 0.30 ppbv, ranging from 0.06 to 0.73 ppbv (Figure 1). For the two downwind sites, they were higher, ranging from 0.07 to 1.45 ppbv, with a 1.28 ppb mean for San Dimas, and 1.45 ppbv for Riverside (Figure 1). For the three sites, three carbonyls formaldehyde, acetaldehyde and acetone accounted for 47 to 55% of the carbonyls measured.

During phase II, conducted during the summer-fall period, the carbonyls concentrations at the background site (Lompoc) averaged 0.21 ppbv, ranging from 0.05 to 0.68 ppbv (Figure 2). For both Mira Loma and Upland, downwind from Los Angeles, the carbonyl concentrations averaged 0.42 ppbv

and ranged from 0.05 to 1.41 ppbv (Figure 2). Likewise, three carbonyls formaldehyde, acetaldehyde and acetone accounted for 50 to 71% of the carbonyls measured.

The levels of the unsaturated carbonyl methacrolein, produced by the atmospheric oxidation of isoprene, were much higher at the urban sites during the spring-summer period (Figure 1). It is remarkable that the highest level of methacrolein was found in the urban areas, and not at the background site. During the summer-fall period, acetone showed the highest level. The highest levels of the industrial solvent 2-butanone were measured in the urban sites (Figure 1 and 2).

Finally, mean carbonyl levels did not differ much from the spring-summer to the summer-fall season. The sum of the measured carbonyl concentrations was about a factor of two higher at the urban sites.

Figure 1. Mean Carbonyl Concentrations for Atascadero, San Dimas, and Riverside Sampled in 2001 Spring-Summer

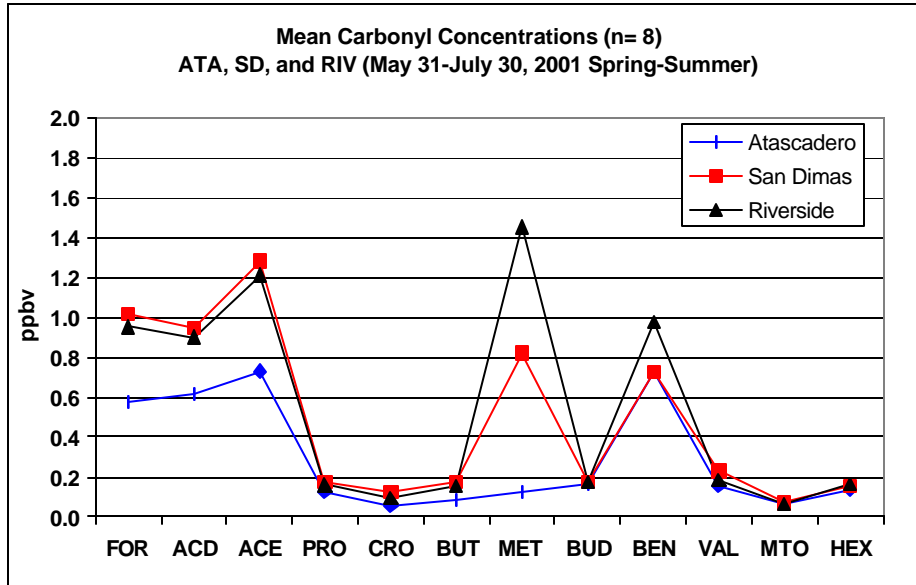
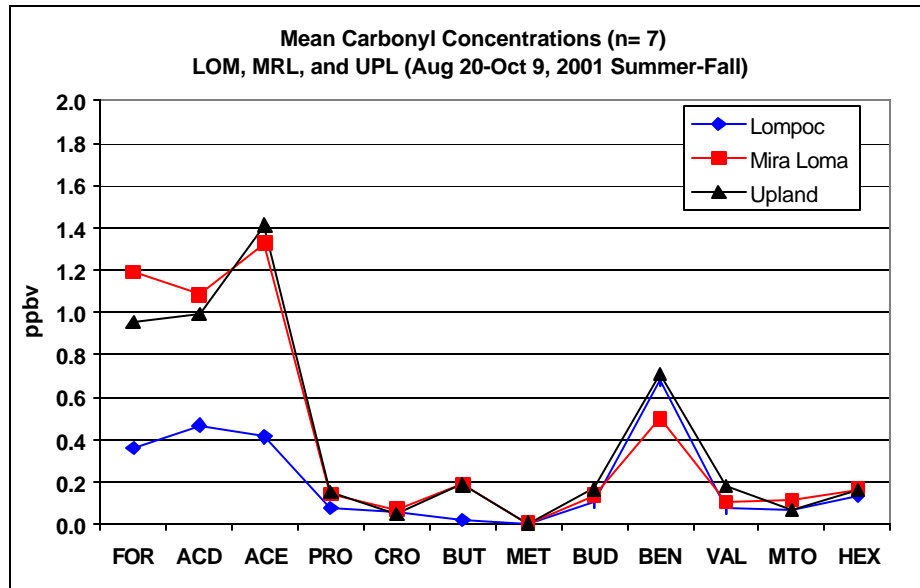


Figure 2. Mean Carbonyl Concentrations for Lompoc, Mira Loma, and Upland Sampled in



2001 Summer-Fall

9. Characterization of PAH and PAH-Derivatives measured with Hi-Vol

The goal of our sampling is to characterize the polycyclic aromatic hydrocarbons (PAH) and PAH-derivatives present at sites chosen to represent source sites or downwind receptor sites and to investigate the atmospheric chemistry occurring at these sites during different seasons. Two types of samples were collected to span the range of volatility of the nitro-PAH: polyurethane foam (PUF) samples for semi-volatile nitro-PAH and filter samples for particle-associated nitro-PAH such as 1-nitropyrene and 2-nitrofluoranthene.

Experimental

Downey, CA

Filter samples. Particulate samples collected at Rancho Los Amigos Hospital in Downey have now been extracted and analyzed by gas chromatography/mass spectrometry (GC/MS) analysis for nitro-PAH. An exploratory analysis of one of the Downey particulate samples was made to determine approximate concentrations of 1-nitropyrene and 2-nitrofluoranthene and to determine appropriate concentrations of deuterated nitro-PAH internal standards for the present analysis. The low levels of these compounds found in the exploratory sample indicated that compositing three particulate samples would be necessary. Three 12-hour daytime samples (0700-1900 hours) were composited to yield one daytime sample and the three corresponding night samples (1900-0700 hours) were composited to yield one nighttime sample. The table below shows the compositing method and the air sampling volumes for the samples.

Sample (Total volume)	Date Sampled	Time Sampled (PST)	Volume (m ³)
Day (1224 m ³)	11/2/00	0700-1900	408
	11/30/00	0700-1900	408
	1/4/01	0700-1900	408
Night (1201 m ³)	11/2-3/00	1914-0700	400
	11/30-12/01/00	1912-0700	401
	1/4-5/01	1910-0700	400

Each of the six 8" x 10" Teflon-impregnated glass fiber filter samples was spiked with the deuterated internal standards 1-nitropyrene-d₉ (50 ng) and 2-nitrofluoranthene-d₉ (250 ng) and placed in a Soxhlet apparatus and extracted for 20 hr with 200 ml dichloromethane (DCM). Each of the six extracts was reduced to 2 ml in a rotary evaporator, filtered (0.2μ), and reduced to 100 μl in a gentle stream of dry nitrogen. Each extract was separated by normal phase high performance liquid chromatography (HPLC) on a silica column (250 x 10 mm, 5μ silica, Regis Chemical Company). The HPLC mobile phase program was as follows: 0-10 min--Hexane; 10-15 min 95% hexane, 5% DCM;

15-40 min--linear gradient to DCM; 40-50 min--DCM; 50-60 min--linear gradient to acetonitrile; 60-70 min--acetonitrile). The nitro-PAH fractions (24-37 min) were composited as noted in the table and reduced by rotary evaporation to 1 ml and under nitrogen to 50 μ l prior to GC/MS analysis.

GC/MS analysis was conducted using a 60 m DB-17 column which allowed resolution the nitro fluoranthene and nitropyrene peaks. Analysis was by selected ion monitoring of the molecular ion and characteristic fragments ions of the nitrofluoranthenes and nitropyrenes (247, 217, 201, 200, and 189) and the corresponding ions for the deuterated species (256, 226, 210, 208 and 198).

PUF samples. Concurrently with the particulate collections in Downey, high-volume vapor-phase samples were collected on polyurethane foam solid adsorbent cylinders (PUF plugs) placed downstream of the filters in the hi-vol sampling train. Each PUF plug was in turn backed up by a back PUF to check for breakthrough.

Prior to extraction, each PUF plug was spiked with a deuterated internal standard solution containing 1-nitronaphthalene-d₇, phenanthrene-d₁₀, fluoranthene-d₁₀, and pyrene-d₁₀. Each PUF sample was separated by the same HPLC method as above. The samples have been pooled according to the above scheme to yield one day sample and one night sample representing the same air sample volumes as the particulate samples. Currently the samples are ready for concentration to 50 μ l prior to GC/MS analysis. The internal standard amounts are given in the following table.

Compound	Front PUFs Day and Night	Back PUFs Day and Night
1-Nitronaphthalene-d ₇	337.9 ng	168.9 ng
Fluoranthene-d ₁₀	5.012 µg	2.506 µg
Pyrene-d ₁₀	4.314 µg	2.157 µg
Phenanthrene-d ₁₀	21.35 µg	10.67 µg

Riverside, CA

Filter samples. During August, three nighttime ultra-high volume particulate samples were taken on nights following afternoons where the ozone peak reached ~150 ppbv. The goal was to isolate air samples modified by evening nitrate radical chemistry. The samples were taken using a "Mega Sampler" equivalent to 16 Hi-Vol samplers that is set up at Riverside. The MegaSampler has been modified by researchers at the Desert Research Institute with 2.5 µm cutoff impactors and collects particles on four 16" x 20" Teflon-impregnated glass fiber filters (TX40HI20,Pallflex). Vapor-phase samples were taken concurrently on PUF plugs downstream of 8"x 10" filters in two modified Hi-Vol samplers.

Exploratory analyses were undertaken on a portion of each MegaSampler filter sample. One filter from each night was spiked with deuterated 2-nitrofluoranthene-d₉ and 1-nitropyrene-d₉ as internal standards, Soxhlet-extracted and chromatographed by HPLC according to the same method used for the Downey samples. The samples are summarized in the following table along with internal standard amounts. The samples were analyzed by GC/MS as noted above.

Sample Code	Date Sampled	Time (PDT)	Sample Volume (m ³)	Total 2-NFl-d ₁₀ (µg)	Total 1-NPy-d ₁₀ (µg)
M01-001	8/18-19/01	1900-0701	3410	0.750	0.150
M01-005	8/25-26/01	1852-0701	3412	2.50	0.500
M01-009	8/26-27/01	1900-0700	3357	0.750	0.150

PUF Samples. Hi-vol PUF samples taken concurrently with MegaSampler filter sample M01-009 (8/26-27/01) have been extracted and are in the process of HPLC separation in preparation for GC/MS analysis. The samples are being worked up in the same way as the Downey PUF samples

except that the internal standards amounts were reduced by a factor of three in anticipation of lower nitro-PAH levels as seen in the Riverside particulate samples relative to the Downey ones.

Results

Nitro-PAH are emitted from combustion sources such as diesel exhaust. The specific nitro-isomers in emissions are those formed by electrophilic nitration, for example, 1-nitropyrene and 3-nitrofluoranthene. Nitro-PAH can be formed by gas-phase atmospheric reactions of the parent PAH with the hydroxyl (OH) radical during the daytime or with the nitrate (NO₃) radical at night, and these radical-initiated reactions often produce nitro-PAH isomers distinct from those directly emitted. For example, 2-nitrofluoranthene is formed from the gas-phase reaction of fluoranthene with either OH radicals or NO₃ radicals. The OH radical-initiated reaction of pyrene produces 2-nitropyrene, while the comparable NO₃ radical reaction with pyrene does not produce significant nitro-derivatives.

The following table lists the 2-nitrofluoranthene and 1- and 2-nitropyrene concentrations measured at Downey and at Riverside. 2-Nitrofluoranthene was the most abundant of the four-ring nitro-PAH at both sites and the concentrations measured were comparable. (It is anticipated that the PAH at Riverside will be significantly lower than at the heavily diesel traffic-impacted site at Downey, and analysis of fluoranthene and pyrene is planned to confirm this). Notable at Riverside was the lack of detectable nitropyrenes. The nondetectable 1-nitropyrene is consistent with dilution occurring at this downwind site, while the lack of 2-nitropyrene suggests that the observed 2-nitrofluoranthene was formed from NO₃ radical-initiated chemistry. We are presently analyzing the semi-volatile nitro-PAH, which should also reflect formation by NO₃ radical chemistry. In particular, the relative abundances of the methylnitronaphthalenes can be used as a "marker" to distinguish NO₃ radical-initiated formation from OH radical formation.

Site	Date	Hours	Concentration (pg m ⁻³)		
			2-Nitro-fluoranthene	1-Nitro-pyrene	2-Nitro-pyrene
Downey	day composite	0700-1900	90	30	27
Downey	night composite	1900-0700	72	60	36
Riverside	8/18-19/01	1900-0700	52	not detected	not detected
Riverside	8/25-26/01	1900-0700	50	not detected	not detected
Riverside	8/26-27/01	1900-0700	79	not detected	not detected

10. Size Distribution And Diurnal Characteristics Of Particle-Bound Metals In Source And Receptor Sites Of The Los Angeles Basin

Correlations between trace elements and metals with similar sources or origin

PM species from similar sources or origin should be highly correlated, given that variability in their concentrations should be attributed to the variability in the emission strengths of their common source. Based on our data from the 24-hour averaged field measurements, we attempted to identify sub-groups of metals and elements in each of the coarse, fine and ultrafine PM modes whose 24-hour concentrations are highly correlated.

The discussion for each of the two sites –Downey and Riverside is presented below.

Downey

Figure 1 shows a plot between 24 hour averaged Si concentrations versus Ti, K, Mn, Fe and Ca concentrations in coarse mode at Downey. Si, which is a crustal metal mostly originating from soil resuspension, has been separately plotted against the other five metals. The data clearly show a very high degree of correlation between the ambient coarse concentrations of Si and those of Ca, Ti, Mn, Fe and K, with correlation coefficients (R^2) ranging from 0.75 to 0.98. In addition to the metals plotted in Figure 1, the coarse PM concentrations of Si and V were also highly correlated ($R^2=0.77$), but V concentrations were not plotted because they are considerably lower than those of any other metal in this mode and are below the resolution of this Figure. The high degree of correlation between the metals of this group and their high relative mass in the coarse mode highly suggests that, at least, the coarse PM mode of Si, Ca, Ti, Mn, Fe, V and K originate from resuspension of soil dust.

Three highly correlated groups of metals and trace elements were identified in the fine and ultrafine PM modes in Downey (Figure 2 and 3). Figure 2a presents four separate scatter plots of the 24-hour averaged ambient $PM_{2.5}$ for Fe versus that of Zn, Mn, Ti, and Pb. The concentrations of these metals are highly correlated, with R^2 varying from 0.77 to 0.80. In the fine PM mode, Fe and Ti are dominated by super micrometer particles suggesting that soil dust resuspension may be the main source for these metals. Zn has been attributed to tire dust and municipal incineration (Cass and McRae, 1982), whereas virtually all of Pb found in the Los Angeles Basin has been attributed to vehicular emissions of mostly gasoline engines (Hutzincker et al., 1975) The remarkable correlation between Pb and the rest of the three metals, despite the substantial difference in their size distributions (with Pb being partitioned in much finer particles than Fe, Ti or Zn) suggest that vehicular emissions in Downey may be indirectly responsible for the production of Fe, Zn and Ti in the fine PM mode, in the form of resuspended road dust (including tire and paved road dust). It is also of interest to note that, historically, the ratio of the average values of iron to manganese in the South Coast of California has been found to vary from 47:1 to 53:1 (Cass and McRae, 1982; Friedlander, 1973), which is very close to the 50:1 ratio present in fine PM road dust samples (Watson, 1979). By examining the slope of the Mn-Fe regression line in Figure 2a, the average iron-to-manganese concentration ratio in fine PM is 55:1 (i.e., the inverse of 0.018), which is also practically identical to the previously reported values in road dust samples. This finding provides further corroboration to the argument that these metals found in fine PM in Downey originate mostly from road dust.

Figure 2b shows a plot between Pb versus Sn and Ba concentrations in the fine mode at Downey. A high Pb-Sn as well as Pb-Ba correlation ($R^2 = 0.66$ and 0.80 , respectively) is clearly depicted. Since Pb is originating from vehicular pollution, it can be inferred that Sn and Ba also originate from mobile sources of the nearby freeways.

Significant correlations were observed between the concentration of Ni and Cr both in the fine as well as the ultrafine modes, with R^2 of 0.54 and 0.50 , respectively (Figure 3). Nickel has been used as a tracer for fuel oil combustion in source-receptor modeling studies in Los Angeles (Cass and McRae, 1982). Although Cr could be emitted from diverse sources, its high correlation with Ni suggest that in Downey Cr is also emitted by the power plants and refineries of the Long Beach area that are upwind of this location.

Riverside

Like metal concentrations in Downey, significant correlations were observed between ambient coarse concentrations of Al, Si, K, Ca, Fe, Mn and Ti in Riverside. This group of metals is primarily present in coarse particles with percentages varying from 80-90%, thereby suggesting resuspension of windblown dust as the most significant source of these metals in Riverside. This is further supported in separate scatter plots of Ca, Ti, Mn, Fe, K and Al versus Si in the coarse mode at Riverside (Figure 4). Pairing these variables in the coarse mode of PM result in very high correlation coefficients (R^2) (between 0.94 to 0.99). In addition to the metals plotted in Figure 4, the coarse PM concentrations of Si were also highly correlated with those of Cu ($R^2=0.74$) and V ($R^2=0.61$), but Cu and V concentrations were not plotted because they are considerably lower than those of any other metal in this mode and are below the resolution of the Figure. The high degree of correlation between the metals of this group reinforces the hypothesis that, at least in the coarse mode, Si, Ca, Ti, Mn, Fe, K, Al, V and Cu originate from resuspension of windblown dust from nearby deserts.

Unlike metal concentrations in Downey, no significant correlations were observed between any groups of metals in the fine PM mode in Riverside, an observation that further supports the hypothesis of their long-range transport origin. As the air parcels travel eastward in the Los Angeles Basin, they pass over highly polluted areas in which a multitude of local vehicular and industrial sources contribute to the concentration of these metals. Given the variability of these sources in emission rates and diurnal trends, no significant correlation between these metals should be expected, which is consistent with our field results.

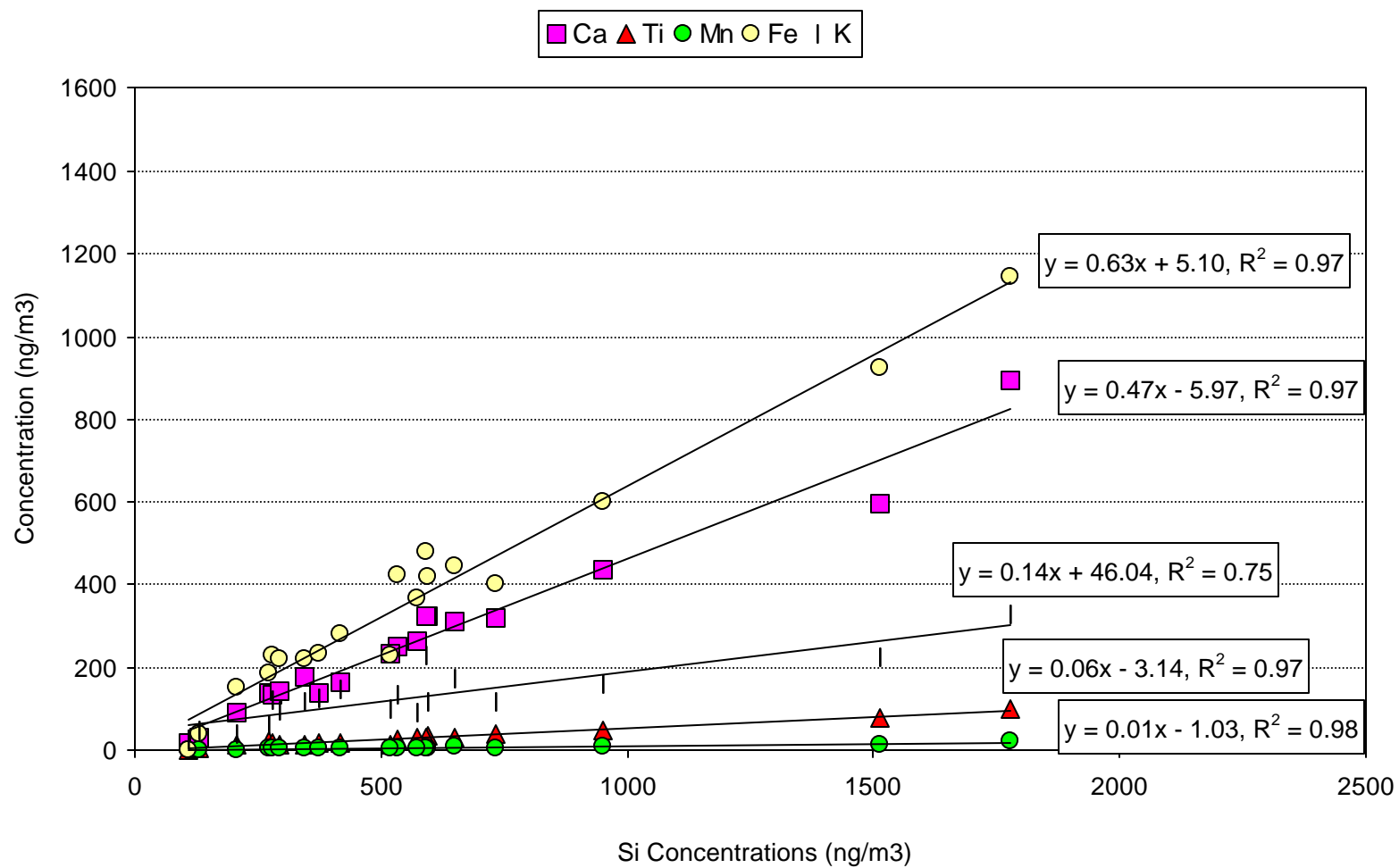


Figure 1. 24-hour averaged Si concentrations versus Ti, K, Mn, Fe and Ca concentrations in coarse PM at Downey.

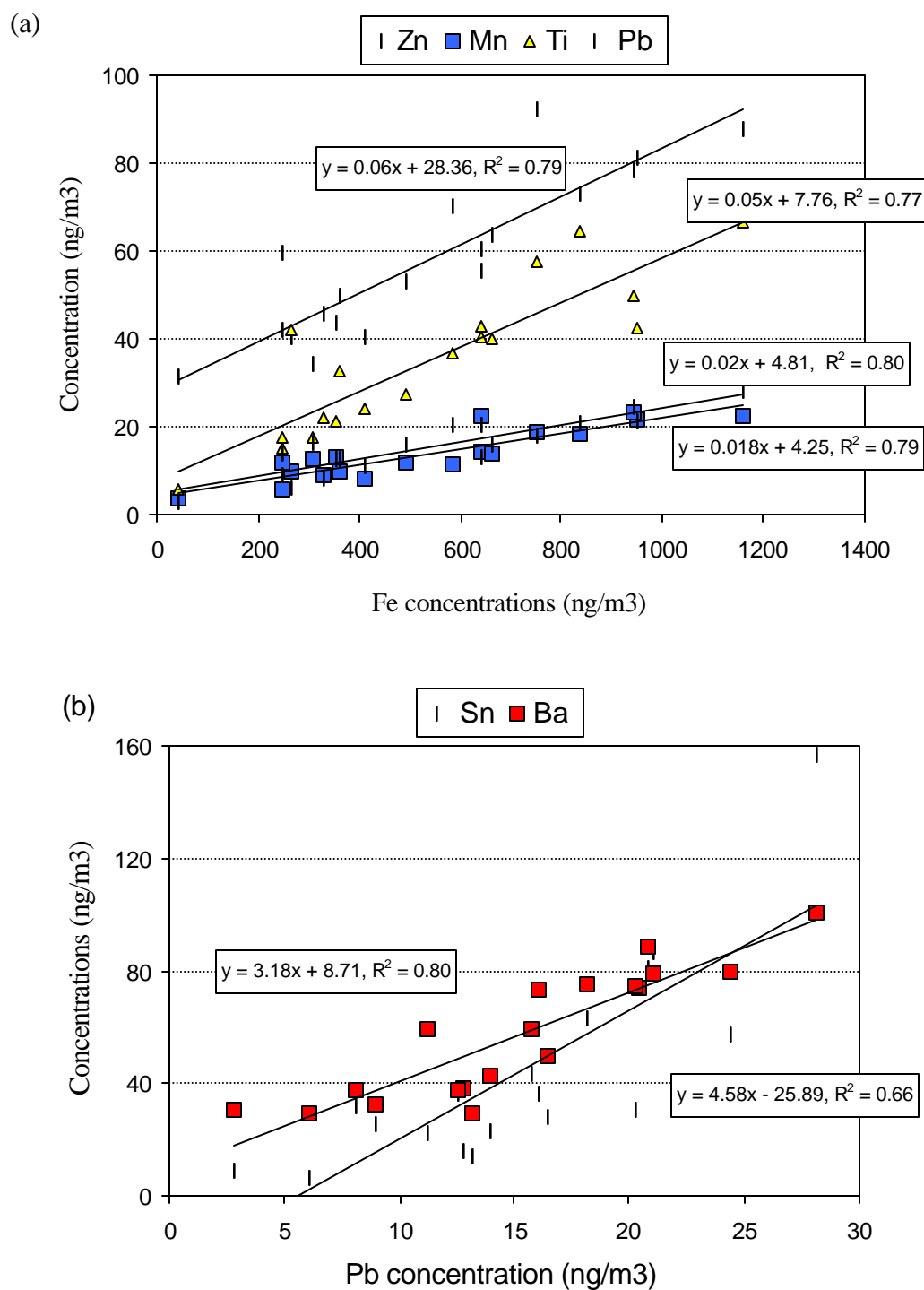


Figure 2. 24-hour averaged (a) Fe concentrations versus Zn, Mn, Ti and Pb concentrations and (b) Pb concentrations versus Sn and Ba concentrations, in Fine PM at Downey.

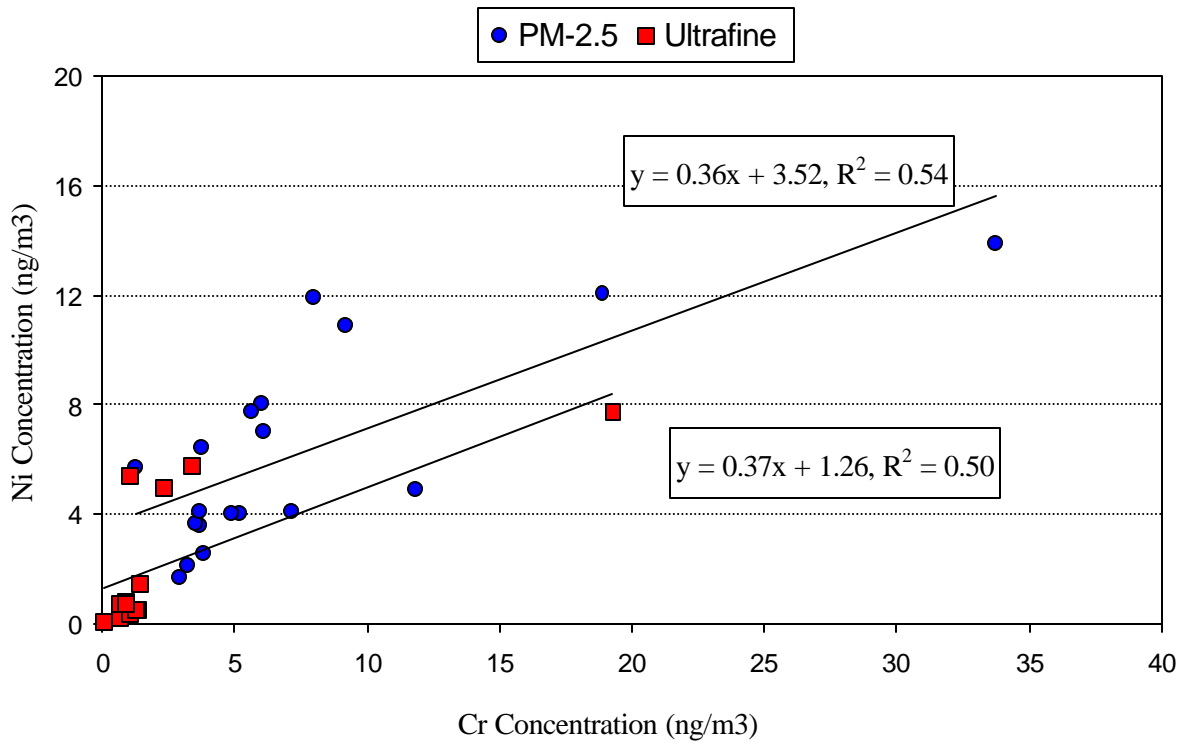


Figure 3. 24-hour averaged Cr versus Ni concentrations in PM_{2.5} and ultrafine PM at Downey.

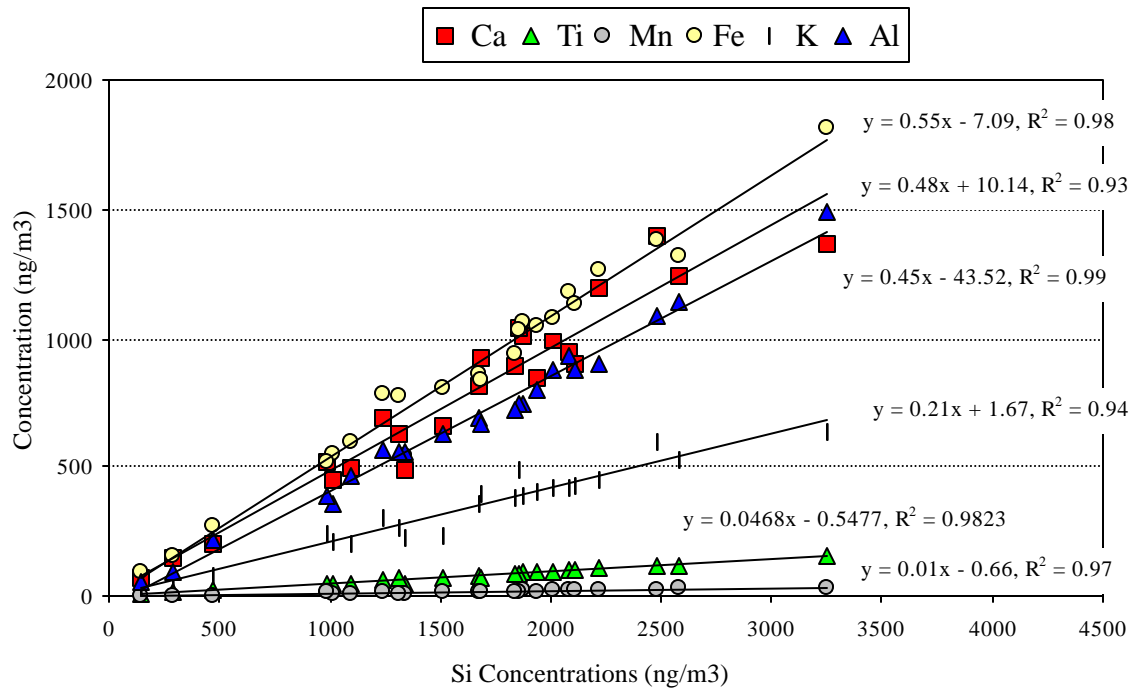


Figure 4. 24-hour averaged Si concentrations versus K, Ca, Ti, Mn, Al and Fe concentrations in coarse PM at Riverside.

11. Ultrafine Particles near 405 Freeway

It is now well established that increases in the concentration of fine particulate matter in urban areas are associated with increases in morbidity and mortality. It is not known what properties of fine particulate matter cause these effects, but one candidate is ultrafine particles. These are particles less than 100 nm or 0.1 μm in size and are found near combustion sources, such as motor vehicles. As a first step to modeling the concentration and size distribution of ultrafine particles in the vicinity of freeways, we have made detailed measurements of ultrafine particles near the 405 freeway, one of the busiest in the country. During the sampling period, traffic density ranged from 140 to 250 vehicles/min passing the sampling site in both directions. Traffic was primarily dominated by gasoline-powered cars and light trucks with less than 5% of vehicles being heavy-duty diesel trucks.

For most of the sampling time, the wind was coming directly from the freeway towards the sampling road with a speed of 1 to 2 m/s. The consistency of observed wind direction and speed is a result of a reliable sea breeze in the sampling area. Consistency of the wind is important for this field experiment, because it allows data from different days to be averaged together.

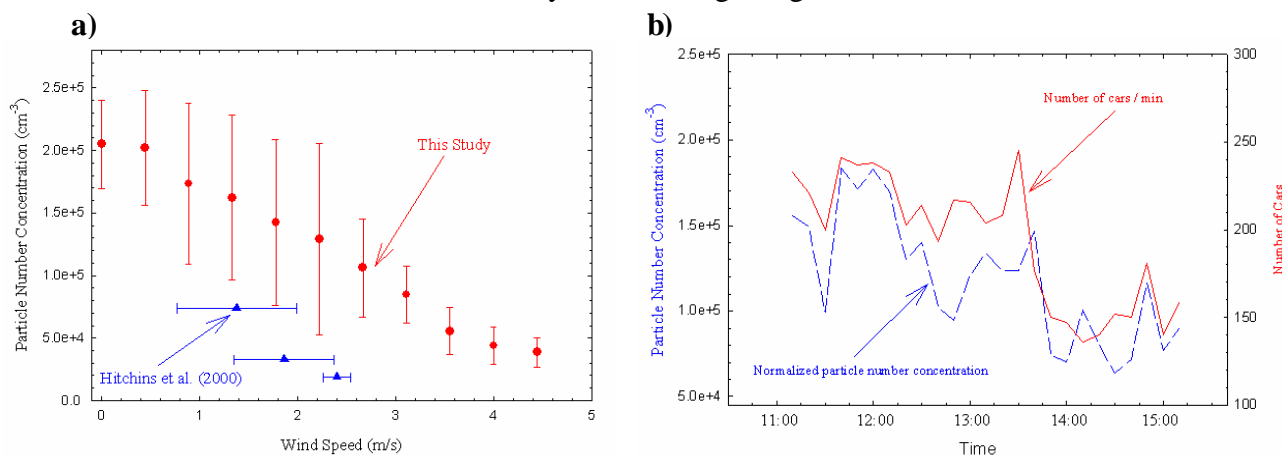


Figure 1: a) Total particle number concentration vs. wind Speed Figure; and b) Traffic Density.

In this study, we found wind direction and speed, played an important role in determining the characteristics of ultrafine particles near the 405 freeway. Figure 1a shows total particle number concentrations as measured by the control CPC, located 30 m downwind of the freeway versus wind speed. Only wind data within 45 degrees of normal to the freeway was used in this figure. This range accounts for more than 80% of the total observations. Data, at 30 m, given by Hitchins et al. (2000) were also included for comparison. It can be seen that total particle number concentration measurements near freeway 405 are in general 2-3 times greater than those observed by Hitchins et al. at Tingalpa, Australia. This is mainly due to the much heavier traffic density on the freeway 405. Although, the absolute particle number concentrations are quite different in these two studies, the relative particle number concentration as function of wind speed are quite similar. This indicates that atmospheric dilution of ultrafine particles by the wind is comparable for both cases.

Figure 1b shows the change in measured particle number concentration and the number of cars passing by the sampling site during those sampling periods when the wind was from the southwest. Since wind speed played an important role in determining the total particle number concentrations, measured CPC readings were normalized to 1 m/s by multiplying the wind speed. As shown in this figure, normalized particle number concentration tracked the traffic density very well indicating that traffic is the major contributor to fine and ultrafine particles. A traffic slowdown on the north bound side of Freeway 405 usually developed around 1:30 pm on a weekday as indicated by the sharp drop of the red curve. During this traffic slowdown, the average vehicle speed is usually less than 5 mph. The control CPC's reading during that time period was observed to be much lower than normal, indicating that fewer ultrafine particles are produced during such traffic slow down.

Particle number concentration and size distribution in the size range from 7 nm to 220 nm were measured by a condensation particle counter (CPC) and a scanning mobility particle spectrometer (SMPS). Measurements were taken at 30 m, 60 m, 90 m, 150 m, 300 m downwind and 300 m upwind from Interstate highway 405 at the Los Angeles National Cemetery. At each sampling point, the concentration of carbon monoxide, black carbon and particle mass were also measured by a Dasibi CO monitor, an Aethalometer and a DataRam, respectively.

The average concentrations of CO, black carbon, particle number and mass concentration at 30 m was in the range of 1.7 to 2.2 ppm, 3.4 to 10.0 $\mu\text{g}/\text{m}^3$, 1.3×10^5 to 2.0×10^5 / cm^3 and 30.2 to 64.6 $\mu\text{g}/\text{m}^3$, respectively.

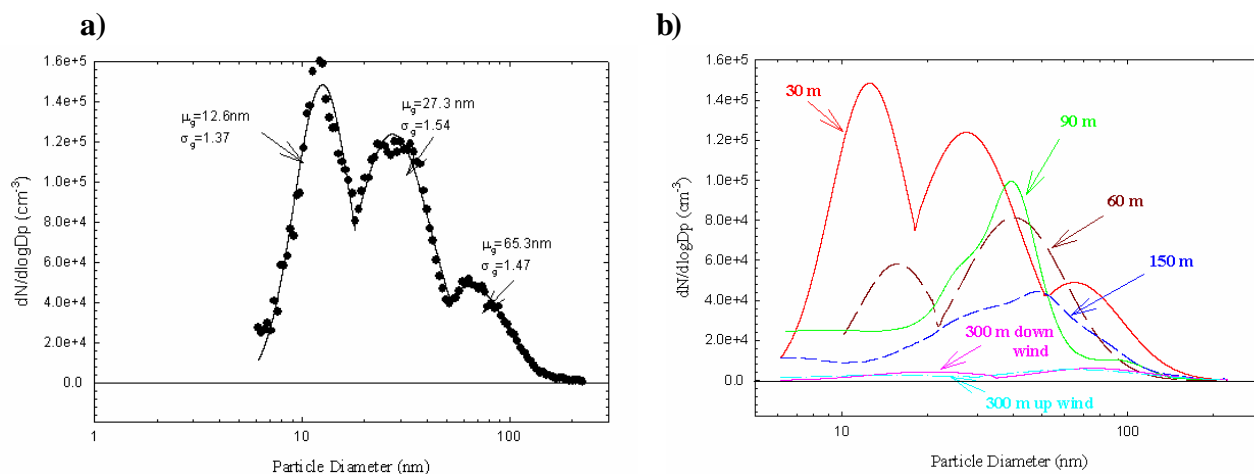


Figure 2. a) Ultrafine Particle Size Distribution at 30 meters Downwind from 405 Freeway; and b) at Different Sampling Locations.

As shown in Figures 2a and 2b, thirty meters downwind from the freeway, three distinct modes were observed with geometric mean diameters of 12.6 nm, 27.3 nm and 65.3 nm, respectively. The smallest

mode, with a peak concentration of $1.6 \times 10^5 \text{ \#/cm}^3$, disappeared at distances greater than 90m from the freeway. The number concentrations for smaller particles, $d_p < 50 \text{ nm}$, dropped significantly with increasing distances from the freeway, but for larger ones, $d_p > 100 \text{ nm}$, number concentrations decreased only slightly. This suggests that coagulation is more important than atmospheric dilution for ultrafine particles and vice versa for large particles. Previously, researchers who conducted experimental and theoretical studies on the transportation and transformation of vehicle particle emission in the atmosphere often concluded that the rapid dilution of the exhaust plume made the coagulation insignificant. However, in the present study, the observed size distribution changes indicate that coagulation is not negligible. Ultrafine particle concentration measured at 300 m downwind of the freeway was indistinguishable from upwind background concentration.

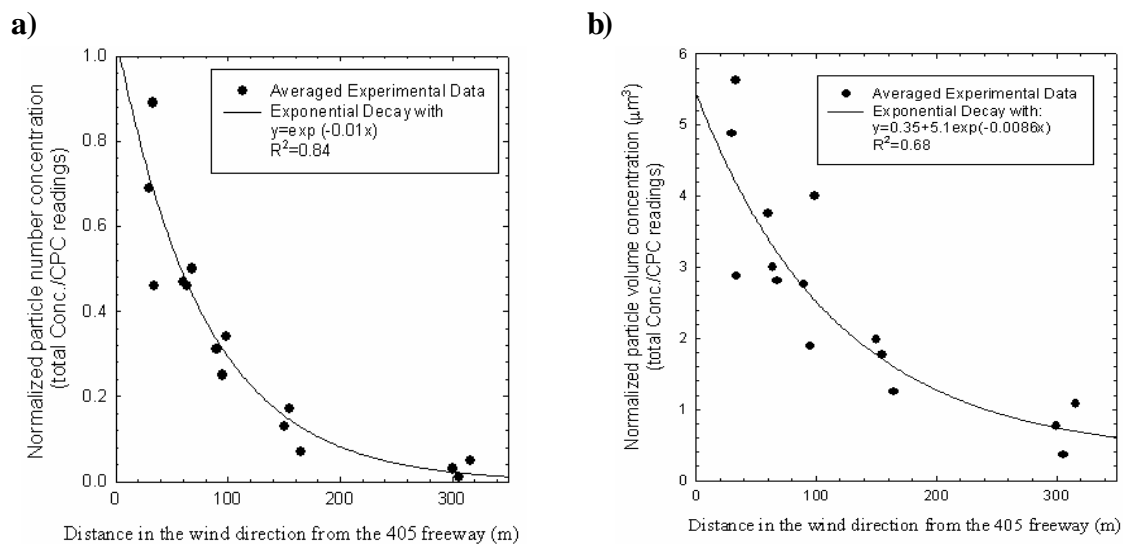


Figure 3. Ultrafine Particle Concentration Vs. Distance from Freeway 405 as a function of a) Number Concentration, and b) Volume Concentration

Figure 3 shows the decay of normalized total particle number and volume concentration, in the size range of 7 nm to 220 nm, respectively, with distance along the wind direction from the freeway. The horizontal axis represents the true distance as an air parcel travels from the freeway to the sampling locations. The total number and volume concentrations were normalized by dividing the averaged total number concentration measured by the control CPC concentration during each sampling periods. Each data point in the figure represents an averaged value for all measurements with the same wind directions. The solid line was the best fitting exponential decay curve. Since coagulation will only decrease the total particle number concentration, not the volume, if coagulation is occurring then, total number concentration will decay faster than total volume concentration, which is the case as shown in Figures 3 (a) and (b).

To make this freeway study more comprehensive, the concentrations of carbon monoxide (CO), black carbon, particle mass, and particle number were also measured at increasing distance from the freeway.

Figure 4 shows the decay curves for relative CO, black carbon, total particle number and mass concentration. The mass concentration decreased only by a few percent throughout the measured range. While, CO, black carbon and particle number concentration decreased about 60% in the first 100 m and then leveled off somewhat after 150 m. In fact, CO, black carbon and particle number concentrations tracked each other extremely well. This observed result confirmed the common assumption that vehicular exhaust is the major source for CO, black carbon and ultrafine particles near a busy freeway. In addition, it suggests that the decreasing characteristics of any of these three pollutants could be used interchangeably to estimate the concentration of the other two pollutants near freeways.

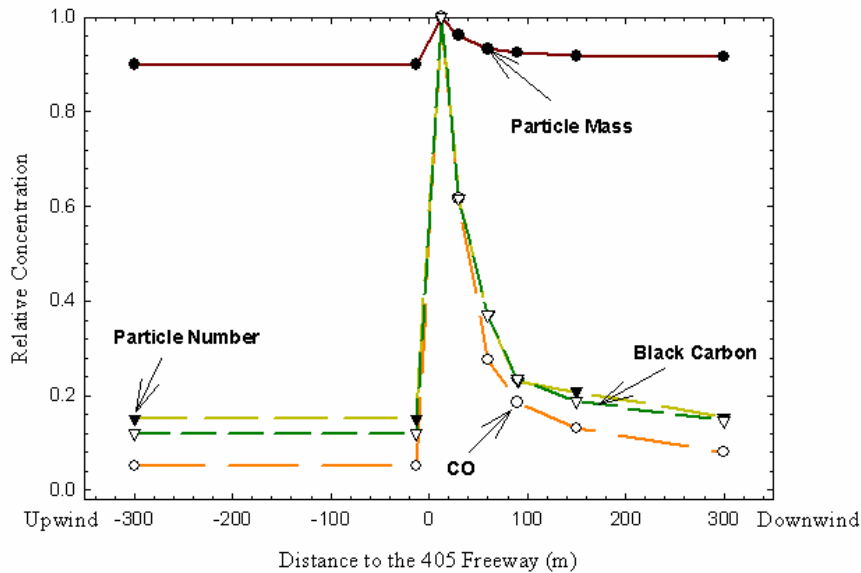


Figure 4. Relative Mass, Number, Black Carbon, CO Concentration near the 405 freeway.

Related future work

Over the next three years we will conduct vertical profiles of ultrafine particle concentration and size distribution and horizontal profiles at locations near other freeways. Currently we are sampling near the 710 freeway, which has a high volume of diesel trucks. Results from this study will be compared with what we have obtained near the 405 freeway, a gasoline vehicle dominated freeway. Similar measurements near the 405 freeway will be conducted in a winter season to study the effect of atmospheric mixing height on the fate of ultrafine particles near a freeway. All these results will be used to develop a model that predicts exposure to ultrafine particles from freeways in terms of traffic density, topography, and meteorology.

12. Investigation of the Relationship between Gas-phase and Aerosol-borne Hydroperoxides in Urban Air

Due to ppb-levels of hydrogen peroxide (H_2O_2) and organic hydroperoxides (ROOH) in ambient air, their high solubility in water, and the presence of a large mass fraction of water in submicron aerosol [1], hydroperoxides might be expected to be present in fine particles at concentrations of the order of 0.1 mM [2]. Given that hydroperoxides decompose rapidly in the presence of metals common in atmospheric aerosols [1], however, it is not clear that hydroperoxides should be present in the aerosol liquid phase. It has been demonstrated that the exposure of respiratory tract cells to H_2O_2 solutions at concentrations ranging from 20 pM to 1 mM results in significant amounts of cell damage [3-5].

Only one previous study of aerosol-phase hydroperoxides has been carried out [6]. In this work, H_2O_2 mass loadings as high as 10 ng m^{-3} were reported in clean continental air at Niwot Ridge, Colorado. A study of "reactive oxygen species" as equivalent H_2O_2 in size-segregated aerosols has also been made [7] in urban air, but this study was likely subject to significant artifacts due to the sample extraction method [8].

Experimental

Samples were collected during daytime between April and August 2001 on the roof of the Math Sciences Building at UCLA in West Los Angeles (WLA). Meteorological data were acquired using instruments located at the hydroperoxide sampling site. Ozone and NO_x measurements were taken from the South Coast Air Quality Management District (SCAQMD) monitoring station, about 1 km SW of the UCLA site.

Gas-phase hydroperoxides were extracted into the aqueous phase using a helical coil collector, as used in previous laboratory studies by this group [8]. Aerosol samples were collected on 47 mm, 2 μm pore-size Teflon membrane filters (Teflo, Pall Corporation). Total suspended particulate (TSP) samples were collected by drawing 110 L min^{-1} of ambient air through the filters (supported on stainless steel filter holders) for six hours. Size segregation of the coarse and fine aerosol was achieved using a virtual impactor, with a 50% cut point at 2.5 μm , described in greater detail by Kim et al. [9]. Aerosols were generated in the lab to verify the stability of hydroperoxides during collection, and field blanks verified artifact-free aerosol collection. The aerosol-phase hydroperoxides were extracted into the aqueous phase by wetting the filters with 0.2 mL of ethanol, and then adding 3 mL of stripping solution. Quantification of the hydroperoxides present in aqueous solution was achieved using an HPLC-fluorescence technique, as described in detail in [8].

Results

In both the gas- and the aerosol-phase, H_2O_2 accounts for the majority of the total of hydroperoxides present. Measured gas- and aerosol-phase concentrations of hydrogen peroxide are shown in Figure 1. In all cases, more than 99.9 % of total ambient H_2O_2 was found to be in the gas-phase. $\text{H}_2\text{O}_{2,\text{gas}}$ concentrations were found to be in the range 0.6-3.3 ppb. $\text{H}_2\text{O}_{2,\text{gas}}$ levels increased from an average of around 1 ppb in early May to 3 ppb in early August. A strong negative correlation between NO_x and H_2O_2 was observed ($R^2 = 0.42$, $P = 0.008$ for a linear fit to a plot of $[\text{H}_2\text{O}_{2,\text{gas}}]$ versus $1/[\text{NO}_x]$).

Ambient $\text{H}_2\text{O}_{2,\text{gas}}$ was uncorrelated with O_3 ($R^2=0.02$) and possibly weakly correlated with relative humidity ($R^2=0.12$, $P = 0.19$) over a limited range (65-85%).

In the period between May and August, H_2O_2 (particulate, PM) mass loadings ranged from $< 0.1 - 13 \text{ ng m}^{-3}$ (Figure 1). This range of values is in broad agreement with the only previous measurements of this quantity [6]. The reactive oxygen species (ROS) measured by Hung and Wang [7] are significantly higher than ours, despite the fact that the aerosol masses they measured ($10\text{-}200 \text{ }\mu\text{g/m}^3$) are similar to those typical for Los Angeles [10]. There are several possible explanations for this, among them the use of ultrasonication in the extraction step used by Hung and Wang [7]. We found that significant levels of H_2O_2 were formed in pure water upon sonication. Virtual impactor samples collected in July and August demonstrate that a significant fraction (25-70%) of the total H_2O_2 mass loading is in the fine aerosol ($\text{PM}_{2.5}$) mode (Figure 1).

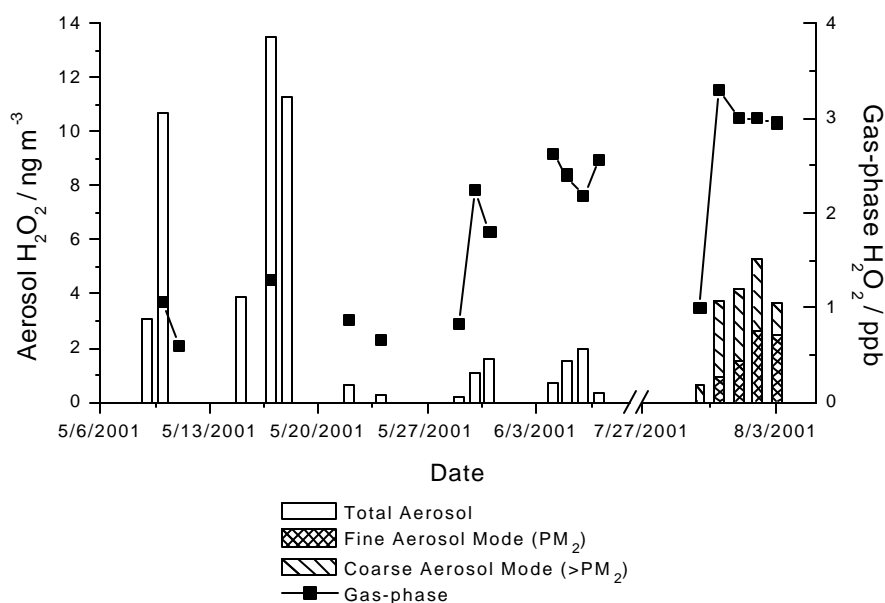


Figure 1 – Ambient H_2O_2 Measurements May-August 2001.

Discussion

To establish whether or not the $\text{H}_2\text{O}_{2,\text{PM}}$ mass loading is in line with Henry's law predictions, it is necessary to know the aerosol mass loading of water. Unfortunately, this parameter could not be measured during the study. We can, however, consider the Henry's law behavior using an upper limit of about $50 \text{ }\mu\text{g m}^{-3}$ aerosol liquid water. This number is based on an upper limit for aerosol mass loadings in West Los Angeles of $< 100 \text{ }\mu\text{g m}^{-3}$; 24 hour average values for TSP in the mid 1990's were typically $60 \text{ }\mu\text{g m}^{-3}$ [10], and observations that water comprises less than 50 % of the total mass of Los Angeles aerosol at $\text{RH} < 80 \%$ [11]. Figure 2 shows a Henry's law plot of $[\text{H}_2\text{O}_2]_{\text{aq}}$, calculated from measurement data by assuming that $50 \text{ }\mu\text{g/m}^3$ of aerosol liquid water for all sampling days vs. $[\text{H}_2\text{O}_2]_{\text{gas}}$. Also included in Figure 2 is the expected relationship between gaseous and aqueous H_2O_2 concentrations given that H_A is $1 \times 10^5 \text{ M atm}^{-1}$ [1]. The calculated lower limits for $[\text{H}_2\text{O}_2]_{\text{aq}}$ are clearly

several times larger than its H_A equilibrium values. Further, the aerosol-phase hydrogen peroxide concentrations, 10^{-3} - 10^{-4} M, are well within the level that damages respiratory tract cells and may be explain a portion of aerosol-associated health effects.

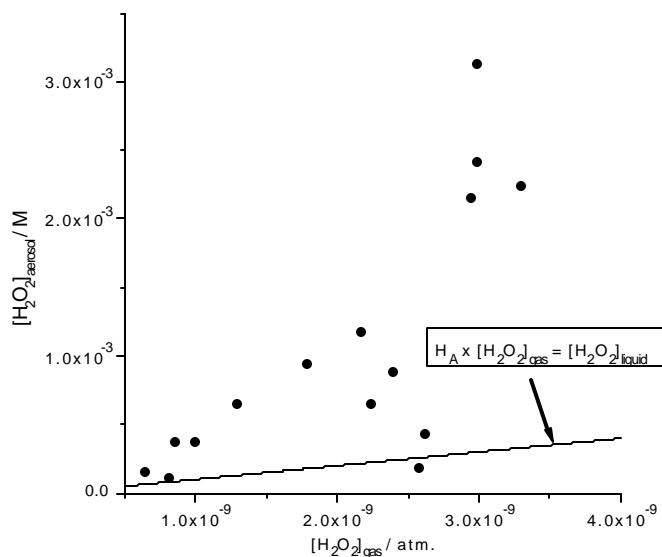


Figure 2 – Henry's Law Plot (Assuming $50 \mu\text{g m}^{-3}$ Liquid Water).

References

1. Seinfeld, J.H. and S. Pandis, Atmospheric Chemistry and Physics. 1997, New York: Wiley Interscience
2. Friedlander, S.K. and E.K. Yeh (1998) Appl. Occup. Environ. Hyg., 13: 416-420.
3. Crim, C. and W.J. Longmore (1995) Am. J. Physiol., 12: L129-L135.
4. Hyslop, P.A., D.B. Hinshaw, J. Halsey, W. A., I.U. Schraufstatter, R.D. Sauerheber, R.G. Spragg, J.H. Jackson, and C.G. Cochrane (1988) J. Biol. Chem., 263: 1665-1675.
5. Simon, R.H., J.A. Edwards, M.M. Reza, and R.G. Kunkel (1991) Am. J. Physiol., 260: L318-L325.
6. Hewitt, C.N. and G.L. Kok (1991) J. Atmos. Chem., 12: 181-194.
7. Hung, H.F. and C.S. Wang (2001) J. Aer. Sci., 32: 1201-1211.
8. Hasson, A.S., G.E. Orzechowska, and S.E. Paulson (2002) *J. Geophys. Res. D, Accepted*
9. Kim, S., Chang, M.C. and Sioutas, C. (2000) *Inhal. Toxicol.*, 12:121-137.
10. California Air Resources Board (1993-1994) California Air Quality Data Vol. XXV-XXVI, No. 1-4.
11. Zhang, X.Q., P.H. McMurry, S.V. Hering, and G.S. Casuccio (1993) Atmos. Environ., 27: 1593-1607.

13. Quality Assurance Audit Report, Claremont, November 2001

Audit Dates: November 6, 2001
Instrumentation Audited: SMPS, APS, DataRAM, Aethalometer, Interior Temperature/RH, Ambient Temperature/RH, Wind Speed, Wind Direction

The purpose of this summary is to provide a report of significant audit findings. The audits were follow-ups to audits conducted March and April 2001 while the PIU was at the Riverside location. Results of the performance audit comparisons are included.

General Status Comments:

1. QAPP: the Supersite Quality Assurance Officer submitted an electronic copy of the final version, including the signature page, to the EPA in early October 2001.
2. System audit of Supersite laboratory: No significant problems noted. The final report is in the process of being completed.
3. System audit of SCPCS data management center: In general, it has been suggested that a true relational database data management environment replace the current spreadsheet format being used

PIU Audit Procedures

The audits consisted of both a system and a performance component. A technical systems audit was conducted to verify that procedures are being followed according to established SOPs. The audit was conducted using a systems audit checklist. The checklist was completed during the March/April 2001 audit. Therefore, the system audit for this audit consisted of a review of the previously completed checklist, concentrating on any changes in procedures and equipment since the last audit. In particular, the operation of the API continuous nitrate and carbon analyzers was reviewed. A siting audit was also conducted to evaluate the representativeness of the site location, checking probe exposures and local sources.

Performance audits were conducted to evaluate the accuracy of the measurements by comparing instrument performance against known standards. NIST-traceable standards were used whenever possible. All standards are maintained independently from standards used at the PIU

Since the majority of the measurements made at the PIU are of particulate matter, the majority of the performance checks consisted of flow measurements using a Gilibrator 2 automated optical bubble flow meter. When possible, flow measurements were made both at the sample train inlet and at the inlet to the sampler in order to verify that the sample train was not damaged in any way during relocation. Similarly, during auditing of the meteorological sensors, emphasis was placed on verifying the orientation of the wind direction sensor, as this too can be altered during relocation.

It happened that the day of the audit was also a sampling day for the PIU. Therefore, in order to avoid any possibility of invalidating any of the 24-hour samplers, no filter samplers were audited during this audit. However, it was confirmed that the same flow standards currently in use were the same used at the time of the previous audit. Since no significant problems in flows were noted during the previous audit, reaudit of these samplers was not considered essential.

In general, the operation of the PIU appears to be going smoothly, with only the relatively minor issues noted below. Problems noted during the audit were discussed with key PIU operating personnel at the time of the audit. Whenever possible, problems were investigated and resolved at the time of the audit.

Key siting AUDIT Findings

The inlet for the IC MOUDI was located approximately 0.3 meters from the surface of a pump box for a sampler located on the roof of the PIU. In addition, the inlet was located approximately 0.5 meters from the exhaust port of the same pump box. Two carbon-vane pumps were located in the pump box. In this configuration, the pump box is a potential source of particulates for the MOUDI. The MOUDI inlet was rotated 180° (hanging over the edge of the PIU) and the pump box was repositioned in order to minimize any **possible impact on the sampler**.

Key SYSTEM AUDIT Findings

As stated in the previous audit, certification procedures for the rotameters used to measure sample flow rates are currently not well established or documented. SOPs for certifying flow measurement devices should be documented, including procedures for maintaining certification documentation. This is a necessary step to assure the traceability of the particulate data. Flows measuring devices should be recertified on at least an annual basis. It is recommended that certification documentation be maintained at the PIU. This documentation could consist simply of a signed and dated sticker on the flow device. Please note that flow meters used for certification should be NIST-traceable to within $\pm 2\%$.

Key Surface Meteorology Audit Results

1) Unless otherwise noted, all instruments were operating within the recommended criteria.

The alignment of the wind directions sensor was 180° out of phase. The sensor mounting appeared to be set up correctly, with the appropriate markings on the sensor body oriented south. A review of the data by project personnel appears to indicate that the problem has only affected data since the PIU's move to Claremont. However, the site technician could not think of anything that had been done differently in setting up the system at Claremont. One possible explanation is that the vane had for some reason been removed from its mount and accidentally reinstalled in the opposite direction. The extent of the problem should be investigated and the affected data corrected.

2) The model of wind sensor used at the PIU is not conducive to testing with a constant RPM motor without disassembling the sensor and jeopardizing the calibration of the wind vane. However, it was possible to confirm the operation of the wind speed sensor "reed switch" and the proper ranging of the readings, confirming the operation of the sensor.

3) The station interior temperature sensor was reading 7° C high. While the station temperature reading is not critical, it is unclear whether or not the system is operating correctly. The system should be recalibrated, and repaired if necessary.

Key Air Quality Audit Findings

When the auditor first checked the flow leading from the TSI 3080 SMPS to the TSI 3022A condensation particle counter, a flowrate of 0.120 lpm was noted. This differed from the 0.3 lpm measured at the inlet of the 3022A. A “tee” was located at the 3022A inlet, with one end leading to the SMPS and the other leading to a valved HEPA filter. The valve was partially opened, and it was confirmed that the rest of the flow (about 0.2 lpm) was being drawn through the HEPA filter. The auditor then shut the valve at the HEPA filter, at which point the flow from the SMPS to the 3022A increased predictably to 0.301 lpm. Since the auditor and the site technician were uncertain as to the correct configuration, the valve at the HEPA filter was again opened in order to obtain the original 0.120 lpm flow rate from the SMPS to the 3022A. Later discussion with project personnel revealed that the valve should have been closed. The period during which the valve was opened should be determined, and the data collected during the period adjusted to compensate for dilution by the filtered air.